Robust Decentralized Secondary Frequency Control in Power Systems: Merits and Tradeoffs

Erik Weitenberg, Yan Jiang, Changhong Zhao, *Member, IEEE*, Enrique Mallada, *Member, IEEE*, Claudio De Persis, and Florian Dörfler

***Abstract*—Frequency restoration in power systems is conventionally performed by broadcasting a centralized signal to local controllers. As a result of energy transition, technological advances, and scientific interest in distributed control and optimization methods, a plethora of distributed frequency control strategies have been proposed recently, which rely on communication amongst local controllers. In this paper, we propose a fully decentralized leaky integral controller for frequency restoration, which is derived from a classic lag element. We study steady-state, asymptotic optimality, nominal stability, input-to-state stability, noise rejection, transient performance, and robustness properties of this controller in closed loop with a nonlinear and multivariable power system model. We demonstrate that the leaky integral controller can strike an acceptable tradeoff between performance and robustness as well as between asymptotic disturbance rejection and transient convergence rate by tuning its dc gain and time constant. We compare our findings to conventional decentralized integral control and distributed-averaging-based integral control in theory and simulations.**

***Index Terms*—Decentralized control, power generation control, power system stability.**

Manuscript received April 16, 2018; revised September 17, 2018; accepted November 20, 2018. Date of publication December 3, 2018; date of current version September 25, 2019. The work of E. Weitenberg and C. De Persis was supported in part by the NWO-URSES project ENBARK, the DST-NWO IndoDutch Cooperation on "Smart Grids—Energy management strategies for interconnected smart microgrids" and the STW Perspectief program "Robust Design of Cyber-physical Systems" – "Energy Autonomous Smart Microgrids". The work of Y. Jiang and E. Mallada was supported in part by the NSF under Grant CNS 1544771, Grant EPCN 1711188, Grant AMPS 1736448, and Grant CAREER 1752362, and in part by the U.S. DoE Award DE-EE0008006. The work of C. Zhao was supported in part by ARPA-E under the NODES program under Grant DE-AC36-08GO28308, and in part by the DOE under the ENERGISE program Award DE-EE0007998. The work of F. Dörfler was supported by ETH funds and the SNF Assistant Professor Energy under Grant 160573. Recommended by Associate Editor Prof. Yann Le Gorrec. *(Corresponding author: Florian Dörfler.)*

E. Weitenberg and C. De Persis are with the University of Groningen, Groningen 9712 CP, The Netherlands (e-mail: e.r.a.weitenberg@gmail.com; c.de.persis@rug.nl).

Y. Jiang and E. Mallada are with the Johns Hopkins University, Baltimore MD 21218 USA (e-mail: yjiang@jhu.edu; mallada@jhu.edu).

C. Zhao is with the National Renewable Energy Laboratory, Golden CO 80401 USA (e-mail: changhong.zhao@nrel.gov).

F. Dörfler is with the Automatic Control Laboratory, Swiss Federal Institute of Technology (ETH) Zürich, Zürich 8092, Switzerland (e-mail: dorfler@ethz.ch).

Color versions of one or more of the figures in this paper are available online at http://ieeexplore.ieee.org.

Digital Object Identifier 10.1109/TAC.2018.2884650

I. Introduction

THE core operation principle of an ac power system is to balance supply and demand in approximately real time. Any instantaneous imbalance results in a deviation of global system frequency from its nominal value. Thus, a central control task is to regulate the frequency in an economically efficient way and despite fluctuating loads, variable generation, and possibly faults. Frequency control is conventionally performed in a hierarchical architecture: The foundation is made of the generators' rotational inertia providing an instantaneous frequency response, and three control layers—primary (droop), secondary automatic generation (AGC), and tertiary (economic dispatch)—operate at different time scales on top of it [1], [2]. Conventionally, droop controllers are installed at synchronous machines and operate fully decentralized, but they cannot by themselves restore the system frequency to its nominal value. To ensure a correct steady-state frequency and a fair power sharing among generators, centralized AGC and economic dispatch schemes are employed on longer time scales.

This conventional operational strategy is currently challenged by increasing volatility on all time scales (due to variable renewable generation and increasing penetration of low-inertia sources) as well as the ever-growing complexity of power systems integrating distributed generation, demand response, microgrids, HVdc systems, etc. Motivated by these paradigm shifts and recent advances in distributed control and optimization, an active research area has emerged developing more flexible distributed schemes to replace or complement the traditional frequency control layers.

In this paper, we focus on secondary control. We refer to [3, Section IV-C] for a survey covering recent approaches amongst which we highlight semicentralized broadcast-based schemes similar to AGC [4]–[6] and also highlight distributed schemes based on consensus-based averaging [7]–[12] or primal dual methods [13]–[16], which all rely on communication amongst controllers. However, because of security, robustness, and economic concerns it is desirable to regulate the frequency without relying on communication. A seemingly obvious and often advocated solution is to complement local proportional droop control with decentralized integral control [5], [7], [17]. In theory, such schemes ensure nominal and global closed-loop stability at a correct steady-state frequency, though in practice they suffer from poor robustness to measurement bias and clock drifts [4], [5], [11], [18]. Furthermore, the power injections resulting from decentralized integral control generally do not lead to an efficient allocation of generation resources. A conventional remedy to overcome performance and robustness issues of integral controllers is to implement them as lag elements with finite dc gain

0018-9286 © 2018 IEEE. Personal use is permitted, but republication/redistribution requires IEEE permission.
See http://www.ieee.org/publications_standards/publications/rights/index.html for more information.

Authorized licensed use limited to: Johns Hopkins University. Downloaded on July 10,2020 at 16:04:53 UTC from IEEE Xplore. Restrictions apply.

[19]. Indeed, such decentralized lag element approaches have been investigated by practitioners: Ainsworth and Grijalva [17] provides insights on the closed-loop steady-states and transient dynamics based on numerical analysis and asymptotic arguments, Heidari *et al.* [20] provides a numerical certificate for ultimate boundedness, and Han *et al.* [21] analyzes lead-lag filters based on a numerical small-signal analysis.

Here, we follow the latter approach and propose a fully decentralized *leaky integral controller* derived from a standard lag element. We consider this controller in feedback with a nonlinear and multivariable multimachine power system model and provide a formal analysis of the closed-loop system concerning the following:

1) steady-state frequency regulation, power sharing, and dispatch properties;

2) the transient dynamics in terms of nominal exponential stability and input-to-state stability with respect to disturbances affecting the dynamics and controller;

3) the dynamic performance as measured by the $\mathcal{H}_2$ norm.

All of these properties are characterized by precisely quantifiable tradeoffs—dynamic versus steady-state performance as well as nominal versus robust performance—that can be set by tuning the dc gain and time constant of our proposed controller. We compare our findings with the corresponding properties of decentralized integral control, and we illustrate our analytical findings with a detailed simulation study based on the IEEE 39-bus power system. We find that our proposed fully decentralized leaky integral controller is able to strike an acceptable tradeoff between dynamic and steady-state performance and can compete with other communication-based distributed controllers.

The remainder of this paper is organized as follows. Section II lays out the problem setup in power system frequency control. Section III discusses the pros and cons of decentralized integral control and proposes the leaky integral controller. Section IV analyzes the steady-state, stability, robustness, and optimality properties of this leaky integral controller. Section V illustrates our results in a numerical case study. Finally, Section VI summarizes and discusses our findings.

Key to the analysis of part of the results in this paper (see Section IV-B) is a strict Lyapunov function. A first attempt to arrive at one was made in preliminary work [7]. The current paper is substantially different from [7], as it establishes several novel and stronger results; provides additional context, motivation, and possible implications; and discusses the tradeoffs that arise from the tunable controller parameters.

II. Power System Frequency Control

A. System Model

Consider a lossless, connected, and network-reduced power system with n generators modeled by the swing equations [1]

$$\dot{\theta} = \omega \tag{1a}$$

$$M\dot{\omega} = -D\omega + P^* - \nabla U(\theta) + u \tag{1b}$$

where $\theta \in \mathbb{T}^n$ and $\omega \in \mathbb{R}^n$ are the generator rotor angles and frequencies relative to the utility frequency given by $2\pi 50$ or $2\pi 60$ Hz. The diagonal matrices $M, D \in \mathbb{R}^{n\times n}$ collect the inertia and damping coefficients $M_i, D_i > 0$, respectively. The generator primary (droop) control is integrated in the damping coefficient D_i, $P^* \in \mathbb{R}^n$ is vector of net power injections (local generation minus local load in the reduced model), and $u \in \mathbb{R}^n$ is a control input to be designed later. Finally, the magnetic energy stored in the purely inductive (lossless) power transmission lines is (up to a constant) given by

$$U(\theta) = -\frac{1}{2}\sum_{i,j=1}^{n} B_{ij}V_iV_j\cos(\theta_i - \theta_j)$$

where $B_{ij} \geq 0$ is the susceptance of the line connecting generators i and j with terminal voltage magnitudes $V_i, V_j > 0$, which are assumed to be constant.

Observe that the vector of power injections

$$(\nabla U(\theta))_i = \sum_{j=1}^{n} B_{ij}V_iV_j\sin(\theta_i - \theta_j) \tag{2}$$

satisfies a zero net power flow balance: $\mathbb{1}_n^T\nabla U(\theta) = 0$, where $\mathbb{1}_n \in \mathbb{R}^n$ is the vector of unit entries. In what follows, we also write these quantities in compact notation as

$$U(\theta) = -\mathbb{1}^{\mathrm{T}}\Gamma\cos(\mathcal{B}^{\mathrm{T}}\theta), \quad \nabla U(\theta) = \mathcal{B}\Gamma\sin(\mathcal{B}^{\mathrm{T}}\theta)$$

where $\mathcal{B} \in \mathbb{R}^{n\times m}$ is the incidence matrix [22] of the power transmission grid connecting the n generators with m transmission lines, and $\Gamma \in \mathbb{R}^{m\times m}$ is the diagonal matrix with its diagonal entries being all the nonzero $V_iV_jB_{ij}$s corresponding to the susceptance and voltage.

We note that all our subsequent developments can also be extended to more detailed structure-preserving models with first-order dynamics (e.g., due to power converters), algebraic load flow equations, and variable voltages by using the techniques developed in [7] and [9]. In the interest of clarity, we present our ideas for the concise albeit stylized model (1).

B. Secondary Frequency Control

In what follows, we refer to a solution $[\theta(t), \omega(t)]$ of (1) as a *synchronous solution* if it is of the form $\dot{\theta}(t) = \omega(t) = \omega_{\text{sync}}\mathbb{1}_n$, where ω_{sync} is the synchronous frequency.

Lemma 1 (Synchronization frequency): If there is a synchronous solution to the power system model (1), then the synchronous frequency is given by

$$\omega_{\text{sync}} = \frac{\sum_{i=1}^{n} P_i^* + \sum_{i=1}^{n} u_i^*}{\sum_{i=1}^{n} D_i} \tag{3}$$

where u_i^* denotes the steady-state control action.

Proof: In the synchronized case, (1b) reduces to $D\omega_{\text{sync}}\mathbb{1}_n + \nabla U(\theta) = P^* + u$. After multiplying this equation by $\mathbb{1}_n^{\mathrm{T}}$ and using $\mathbb{1}_n^T\nabla U(\theta) = 0$, we arrive at the claim (3). ■

Observe from (3) that $\omega_{\text{sync}} = 0$ if and only if all injections are balanced: $\sum_{i=1}^{n} P_i^* + u_i^* = 0$. In this case, a synchronous solution coincides with equilibrium $(\theta^*, \omega^*, u^*) \in \mathbb{T}^n \times \{\mathbb{0}_n\} \times \mathbb{R}^n$ of (1). Our first objective is frequency regulation, also referred to as secondary frequency control.

Problem 1 (Frequency restoration): Given an unknown constant vector P^*, we design a control strategy $u = u(\omega)$ to stabilize the power system model (1) to an equilibrium $(\theta^*, \omega^*, u^*) \in \mathbb{T}^n \times \{\mathbb{0}_n\} \times \mathbb{R}^n$ so that $\sum_{i=1}^{n} P_i^* + u_i^* = 0$.

Observe that there are manifold choices of u^* to achieve this task. Thus, a further objective is the most economic allocation of steady-state control inputs u^* given by a solution to the following

Authorized licensed use limited to: Johns Hopkins University. Downloaded on July 10,2020 at 16:04:53 UTC from IEEE Xplore. Restrictions apply.

optimal dispatch problem:

$$\text{minimize}_{u\in\mathbb{R}^n} \quad \sum_{i=1}^{n} a_i u_i^2 \tag{4a}$$

$$\text{subject to} \quad \sum_{i=1}^{n} P_i^* + \sum_{i=1}^{n} u_i = 0\,. \tag{4b}$$

The term $a_i u_i^2$ with $a_i > 0$ is the quadratic generation cost for generator i. Observe that the unique minimizer $u^\star$ of the linearly constrained quadratic program (4) guarantees *identical marginal costs* at optimality [8], [10] as

$$a_i u_i^\star = a_j u_j^\star \quad \forall i,j \in \{1,\dots,n\}\,. \tag{5}$$

We remark that a special case of the identical marginal cost criterion (5) is *fair proportional power sharing* [23] when the coefficients a_i are chosen inversely to a reference power $\bar{P}_i > 0$ (normally the power rating) for every generator i given by

$$u_i^\star/\bar{P}_i = u_j^\star/\bar{P}_j \quad \forall i,j \in \{1,\dots,n\}\,. \tag{6}$$

The optimal dispatch problem (4) also captures the core objective of the so-called *economic dispatch problem* [24], and it is also known as the *base point and participation factors* method [24, Ch. 3.8].

Problem 2 (Optimal frequency restoration): Given an unknown constant vector P^*, we design a control strategy $u = u(\omega)$ to stabilize the power system model (1) to an equilibrium $(\theta^*, \omega^*, u^*) \in \mathbb{T}^n \times \{\mathbb{0}_n\} \times \mathbb{R}^n$ where u^* minimizes the optimal dispatch problem (4).

Besides steady-state optimal frequency regulation, we will also pursue certain robustness and transient performance characteristics of the closed loop that we specify later.

III. Fully Decentralized Frequency Control

The frequency-regulation Problems 1 and 2 have seen many centralized and distributed control approaches. Since P^* is generally unknown, all approaches explicitly or implicitly rely on integral control of the frequency error. In the following, we focus on *fully decentralized* integral control approaches making use only of local frequency measurements: $u_i = u_i(\omega_i)$.

A. Decentralized Pure Integral Control

One possible control action is *decentralized pure integral control* of the locally measured frequency, i.e.,

$$u = -p \tag{7a}$$

$$T\dot{p} = \omega \tag{7b}$$

where $p \in \mathbb{R}^n$ is an auxiliary local control variable, and $T \in \mathbb{R}^{n\times n}$ is a diagonal matrix of positive *time constants* $T_i > 0$. The closed-loop system (1), (7) enjoys many favorable properties, such as solving the frequency-regulation Problem 1 with *global* convergence guarantees regardless of the system or controller initial conditions or the unknown vector P^*.

Theorem 2 (Convergence under decentralized pure integral control): The closed-loop system (1), (7) has a nonempty set $\mathcal{X}^* \subseteq \mathbb{T}^n \times \{\mathbb{0}_n\} \times \mathbb{R}^n$ of equilibria, and all trajectories $[\theta(t), \omega(t), p(t)]$ globally converge to $\mathcal{X}^*$ as $t \to +\infty$.

Proof: This proof is based on an idea initially proposed in [7] while we make some arguments and derivations more rigorous here. First, note that (7) can be explicitly integrated as

$$u = -T^{-1}(\theta - \theta_0) - p_0 = -T^{-1}(\theta - \theta_0') \tag{8}$$

where we used $\theta_0' = \theta_0 - Tp_0$ as a shorthand. In what follows, we study only the state $[\theta(t), \omega(t)]$ without $p(t)$ since $p(t)$ is a function of $\theta(t)$ and initial conditions as defined in (8).

Next, consider the LaSalle function

$$\mathcal{V}(\theta,\omega) = \frac{1}{2}\omega^{\mathrm{T}} M\omega + U(\theta) - \theta^{\mathrm{T}} P^* + \frac{1}{2}(\theta - \theta_0')^{\mathrm{T}} T^{-1}(\theta - \theta_0'). \tag{9}$$

The derivative of $\mathcal{V}$ along any trajectory of (1), (7) is

$$\dot{\mathcal{V}}(\theta,\omega) = -\omega^{\mathrm{T}} D\omega\,. \tag{10}$$

Note that for any initial condition $(\theta_0, \omega_0) \in \mathbb{T}^n \times \mathbb{R}^n$, the sublevel set $\Omega := \{(\theta,\omega) \mid \mathcal{V}(\theta,\omega) \le \mathcal{V}(\theta_0,\omega_0)\}$ is compact. Indeed, Ω is closed because of continuity of $\mathcal{V}$ and bounded since $\mathcal{V}$ is radially unbounded because of quadratic terms in ω and θ. The set Ω is also forward invariant since $\dot{\mathcal{V}} \le 0$ by (10).

In order to proceed, we define the zero-dissipation set as

$$\mathcal{E} = \left\{(\theta,\omega) \mid \dot{\mathcal{V}}(\theta,\omega) = 0\right\} = \{(\theta,\omega) \mid \omega = \mathbb{0}_n\} \tag{11}$$

and $\mathcal{E}_\Omega := \mathcal{E} \cap \Omega$. By LaSalle's theorem [25, Th. 4.4], as $t \to +\infty$, $[\theta(t), \omega(t)]$ converges to a nonempty, compact, invariant set $\mathcal{L}_\Omega$, which is a subset of $\mathcal{E}_\Omega$. In the following, we show that any point $(\theta', \omega') \in \mathcal{L}_\Omega$ is an equilibrium of (1), (7). Owing to the invariance of $\mathcal{L}_\Omega$, the trajectory $[\theta(t), \omega(t)]$ starting from (θ', ω') stays identically in $\mathcal{L}_\Omega$ and thus in $\mathcal{E}_\Omega$. Therefore, by (11) we have $\omega(t) \equiv 0$ and hence $\dot{\omega}(t) \equiv 0$. Thus, every point on this trajectory, in particular the starting point (θ', ω'), is an equilibrium of (1), (7). ■

The astonishing global convergence merit of decentralized integral control comes at a cost though. First, note that the steady-state injections from decentralized integral control (7)

$$u^* = -T^{-1}(\theta^* - \theta_0) - p_0$$

depend on initial conditions and the unknown values of P^*. Thus, in general, u^* does not meet the optimality criterion (5). Second and more importantly, *internal instability* due to decentralized integrators is a known phenomenon in control systems [26], [27]. In this particular scenario, as shown in [11, Th. 1] and [4, Proposition 1], the decentralized integral controller (7) is not robust to arbitrarily small biased measurement errors that may arise, e.g., due to clock drifts [18]. More precisely, the closed-loop system consisting of (1) and the integral controller subject to measurement bias $\eta \in \mathbb{R}^n$

$$u = -p \tag{12a}$$

$$T\dot{p} = \omega + \eta\,, \tag{12b}$$

does not admit any synchronous solution unless $\eta \in \text{span}(\mathbb{1}_n)$, that is, all biases η_i, for all $i \in \{1,\dots,n\}$, are perfectly identical [4, Proposition 1]. Thus, while theoretically favorable, the decentralized integral controller (7) is not practical.

B. Decentralized Lag and Leaky Integral Control

In standard frequency-domain control design [19] a stable and finite dc-gain implementation of a proportional-integral (PI)

Authorized licensed use limited to: Johns Hopkins University. Downloaded on July 10,2020 at 16:04:53 UTC from IEEE Xplore. Restrictions apply.

controller is given by a *lag element* parameterized as

$$\alpha\frac{Ts+1}{\alpha Ts+1} = \underbrace{1}_{\text{proportional control}} + \underbrace{\frac{\alpha-1}{\alpha Ts+1}}_{\text{leaky integral control}}$$

where $T>0$ and $\alpha \gg 1$. The lag element consists of a proportional channel as well as a first-order lag often referred to as a *leaky integrator*. In our context, a state-space realization of a decentralized lag element for frequency control is given by

$$\begin{aligned} u &= -\omega - (\alpha-1)p \\ \alpha T\dot{p} &= \omega - p \end{aligned}$$

where T is a diagonal matrix of time constants, and $\alpha \gg 1$ is scalar. In what follows, we disregard the proportional channel (that would add further droop) and focus on the leaky integrator to remedy the shortcomings of pure integral control (7).

Consider the *leaky integral controller*

$$u = -p \tag{13a}$$

$$T\dot{p} = \omega - K\,p \tag{13b}$$

where $K, T \in \mathbb{R}^{n\times n}$ are diagonal matrices of positive control gains $K_i, T_i > 0$. The transfer function of the leaky integral controller (13) at a node i (from ω_i to $-u_i$) is given by

$$\mathcal{K}_i(s) = \frac{1}{T_i s + K_i} = \frac{K_i^{-1}}{(T_i/K_i)\cdot s + 1} \tag{14}$$

i.e., the leaky integrator is a first-order lag with *dc gain* K_i^{-1} and *bandwidth* K_i/T_i. It is instructive to consider the following limiting values for the gains.

1) For $T_i \searrow 0$, leaky integral control (13) reduces to proportional (droop) control with gain K_i^{-1}.
2) For $K_i \searrow 0$, we recover the pure integral control (7).
3) For $K_i \nearrow \infty$ or $T_i \nearrow \infty$, we obtain an open-loop system without control action.

Thus, from a loop-shaping perspective for open-loop stable single-input-single-output (SISO) systems, we expect good steady-state frequency regulation for a large dc gain K_i^{-1}, and a large (respectively, small) cut-off frequency K_i/T_i likely results in good nominal transient performance (respectively, good noise rejection). We will confirm these intuitions in the next section, where we analyze the leaky integrator (13) in closed loop with the nonlinear and multivariable power system (1) and highlight its merits and tradeoffs as function of the gains K and T.

IV. Properties of the Leaky Integral Controller

The power system model (1) controlled by the leaky integrator (13) gives rise to the closed-loop system

$$\dot{\theta} = \omega \tag{15a}$$

$$M\dot{\omega} = -D\omega + P^* - \nabla U(\theta) - p \tag{15b}$$

$$T\dot{p} = \omega - K\,p\,. \tag{15c}$$

We make the following standing assumption on this system.

Assumption 1 (Existence of a synchronous solution): Assume that the closed-loop (15) admits a synchronous solution $(\theta^*, \omega^*, p^*)$ of the form

$$\dot{\theta}^* = \omega^* \tag{16a}$$

$$\mathbb{0}_n = -D\omega^* + P^* - \nabla U(\theta^*) - p^* \tag{16b}$$

$$\mathbb{0}_n = \omega^* - K\,p^* \tag{16c}$$

where $\omega^* = \omega_{\text{sync}}\mathbb{1}_n$ for some $\omega_{\text{sync}} \in \mathbb{R}$. ■

By eliminating the variable p^* from (16), we arrive at

$$P^* - (D + K^{-1})\,\omega_{\text{sync}}\mathbb{1}_n = \nabla U(\theta^*)\,. \tag{17}$$

Equation (17) takes the form of lossless active power flow equations [1] with injections $P^* - (D+K^{-1})\,\omega_{\text{sync}}\mathbb{1}_n$. Thus, Assumption 1 is equivalent to assuming feasibility of the power flow (17), which is always true for sufficiently small $\|P^*\|$.

Under this assumption, we now show various properties of the closed-loop system (15) under leaky integral control (13).

A. Steady-State Analysis

We begin our analysis by studying the steady-state characteristics. At a steady state, the control input u^* takes the value

$$u^* = -p^* = -K^{-1}\omega^* = -K^{-1}\omega_{\text{sync}}\mathbb{1}_n \tag{18}$$

that is, it has a finite dc gain K^{-1} similar to a primary droop control. The following result is analogous to Lemma 1.

Lemma 3 (Steady-state frequency): Consider the closed-loop system (15) and its equilibria (16). The explicit synchronization frequency is given by

$$\omega_{\text{sync}} = \frac{\sum_{i=1}^n P_i^*}{\sum_{i=1}^n D_i + K_i^{-1}}. \tag{19}$$

Unsurprisingly, the leaky integral controller (13) does not generally regulate the synchronous frequency ω_{sync} to zero unless $\sum_i P_i^* = 0$. However, it can achieve *approximate frequency* regulation within a prespecified tolerance band.

Corollary 4 (Banded frequency restoration): Consider the closed-loop system (15). The synchronous frequency ω_{sync} takes a value in a band around zero, which can be made arbitrarily small by choosing the gains $K_i > 0$ sufficiently small. In particular, for any $\varepsilon > 0$, if

$$\sum_{i=1}^n K_i^{-1} \geq \frac{|\sum_{i=1}^n P_i^*|}{\varepsilon} - \sum_{i=1}^n D_i \tag{20}$$

then $|\omega_{\text{sync}}| \leq \varepsilon$.

While regulating the frequencies to a narrow band is sufficient in practical applications, the closed-loop performance may suffer since the control input (13) may become ineffective because of a small bandwidth K_i/T_i. Similar observations have also been made in [17] and [20]. We will repeatedly encounter this tradeoff for the decentralized leaky integral controller (13) between choosing a small gain K (for desirable steady-state properties) and large gain (for transient performance).

The closed-loop steady-state injections are given by (18), and we conclude that the leaky integral controller achieves proportional power-sharing by tuning its gains appropriately.

Corollary 5 (Steady-state power-sharing): Consider the closed-loop system (15). The steady-state injections u^* of the leaky integral controller achieve fair proportional power-sharing as follows:

$$K_i u_i^* = K_j u_j^* \quad \forall i,j \in \{1,\dots,n\}\,. \tag{21}$$

Authorized licensed use limited to: Johns Hopkins University. Downloaded on July 10,2020 at 16:04:53 UTC from IEEE Xplore. Restrictions apply.

Hence, arbitrary power-sharing ratios, as in (6), can be prescribed by choosing the control gains as $K_i \sim 1/\bar{P}_i$. Similarly, we have the following result on steady-state optimality.

Corollary 6 (Steady-state optimality): Consider the closed-loop system (15). The steady-state injections u^* of the leaky integral controller minimize the optimal dispatch problem as follows:

$$\text{minimize}_{u\in\mathbb{R}^n} \quad \sum_{i=1}^{n} K_i u_i^2 \tag{22a}$$

$$\text{subject to} \quad \sum_{i=1}^{n} P_i^* + \sum_{i=1}^{n}(1+D_iK_i)u_i = 0\,. \tag{22b}$$

Proof: Observe from (21) that the steady-state injections (18) meet the identical marginal cost requirement (5) with $a_i = K_i$. Additionally, the steady-state equations (16b), (16c), and (18) can be merged to the expression

$$\mathbb{0}_n = DK\,u^* + P^* - \nabla U(\theta^*) + u^*\,.$$

By multiplying the left-hand side of this equation by $\mathbb{1}_n^{\mathrm{T}}$, we arrive at condition (22b). Hence, the injections u^* are also feasible for (22) and thus optimal for program (22). ■

The steady-state injections of the leaky integrator are optimal for the modified dispatch problem (22) with appropriately chosen cost functions. From (22b), the leaky integrator does not achieve perfect power balancing $\sum_{i=1}^{n} P_i^* + u_i^* = 0$ and underestimates the net load, but it can satisfy the power balance (4b) arbitrarily well for K chosen sufficiently small. Note that in practice, the control gain K cannot be chosen arbitrarily small to avoid ineffective control and the shortcomings of the decentralized integrator (7) (lack of robustness and power sharing). The following sections will make these ideas precise from the perspectives of stability, robustness, and optimality.

B. Stability Analysis

For ease of analysis, in this section, we introduce a change of coordinates for the voltage phase angle θ. Let $\delta = \theta - \frac{1}{n}\mathbb{1}_n\mathbb{1}_n^{\mathrm{T}}\theta = \Pi\theta$ be the center-of-inertia coordinates (see e.g., [28], [9]), where $\Pi = I - \frac{1}{n}\mathbb{1}_n\mathbb{1}_n^{\mathrm{T}}$. In these coordinates, the open-loop system (1) becomes

$$\dot{\delta} = \Pi\omega \tag{23a}$$

$$M\dot{\omega} = -D\omega + P^* - \nabla U(\delta) + u \tag{23b}$$

where by an abuse of notation we use the same symbol U for the potential function expressed in terms of δ

$$U(\delta) = -\mathbb{1}^{\mathrm{T}}\Gamma\cos\left(\mathcal{B}^{\mathrm{T}}\delta\right), \quad \nabla U(\delta) = \mathcal{B}\Gamma\sin\left(\mathcal{B}^{\mathrm{T}}\delta\right).$$

Note that $\mathcal{B}^{\mathrm{T}}\Pi = \mathcal{B}^{\mathrm{T}}$ since $\mathcal{B}^{\mathrm{T}}\mathbb{1}_n = \mathbb{0}_n$ [22]. The synchronous solution $(\theta^*, \omega^*, p^*)$[1] defined in (16) is mapped into the point $(\delta^*, \omega^*, p^*)$, with $\delta^* = \Pi\theta^*$, satisfying conditions

$$\dot{\delta}^* = \mathbb{0}_n \tag{24a}$$

$$\mathbb{0}_n = -D\omega^* + P^* - \nabla U(\delta^*) - p^* \tag{24b}$$

$$\mathbb{0}_n = \omega^* - K\,p^*. \tag{24c}$$

[1]Of course, care must be taken when interpreting the results in this section since the steady-state itself depends on the controller gain K (see Section IV-A). Here we are merely interested in the stability relative to the equilibrium.

The existence of $(\delta^*, \omega^*, p^*)$ is guaranteed by Assumption 1. Additionally, we make the following standard assumption constraining steady-state angle differences.

Assumption 2 (Security constraint): The synchronous solution (24) is such that $\mathcal{B}^{\mathrm{T}}\delta^* \in \Theta := (-\frac{\pi}{2}+\rho, \frac{\pi}{2}-\rho)^m$ for a constant scalar $\rho \in (0, \frac{\pi}{2})$.

Remark 1: Compared with the conventional security constraint assumption [8], we introduce an extra margin ρ on the constraint to be able to explicitly quantify the decay of the Lyapunov function we use in proofs of Theorems 7 and 8. ■

By using Lyapunov techniques following [12], it is possible to show that the leaky integral controller (13) guarantees exponential stability of the synchronous solution (24).

Theorem 7 (Exponential stability under leaky integral control): Consider the closed-loop system (13) and (23). Let Assumptions 1 and 2 hold true. The equilibrium $(\delta^*, \omega^*, p^*)$ is locally exponentially stable. In particular, given the incremental state

$$x = x(\delta, \omega, p) = \mathrm{col}(\delta - \delta^*, \omega - \omega^*, p - p^*) \tag{25}$$

the solutions $x(t) = \mathrm{col}(\delta(t) - \delta^*, \omega(t) - \omega^*, p(t) - p^*)$, with $[\delta(t), \omega(t), p(t)]$ a solution to (13) and (23) that starts sufficiently close to the origin satisfy for all $t \geq 0$,

$$\|x(t)\|^2 \leq \lambda e^{-\alpha t}\|x_0\|^2 \tag{26}$$

where λ and α are positive constants. In particular, when multiplying the gains K and T by the positive scalars κ and τ, respectively, α is monotonically nondecreasing as a function of the gain κ and nonincreasing as a function of τ.

Proof: Consider the incremental Lyapunov function from [12], including a cross term between potential and kinetic energies, as

$$\begin{aligned} V(x) = {} & \frac{1}{2}(\omega-\omega^*)^{\mathrm{T}}M(\omega-\omega^*) \\ & + U(\delta) - U(\delta^*) - \nabla U(\delta^*)^{\mathrm{T}}(\delta-\delta^*) \\ & + \frac{1}{2}(p-p^*)^{\mathrm{T}}T(p-p^*) \\ & + \epsilon(\nabla U(\delta) - \nabla U(\delta^*))^{\mathrm{T}}M\omega \end{aligned} \tag{27}$$

where $\epsilon \in \mathbb{R}$ is a small positive parameter.

First, we will show that this is indeed a valid Lyapunov function, by proving positivity outside of the origin and strict negativity of its time derivative along the solutions of (23).

For sufficiently small values of ϵ and if Assumption 2 holds, $V(x)$ satisfies condition

$$\beta_1\|x\|^2 \leq V(x) \leq \beta_2\|x\|^2 \tag{28}$$

for some $\beta_1, \beta_2 > 0$ and for all x with $\mathcal{B}^{\mathrm{T}}\delta \in \Theta$, by Lemma 14 in Appendix A. The derivative of $V(x)$ can be expressed as

$$\dot{V}(x) = -\chi^{\mathrm{T}}H(\delta)\chi$$

where $\chi(\delta, \omega, p) := \mathrm{col}(\nabla U(\delta) - \nabla U(\delta^*), \omega - \omega^*, p - p^*)$

$$H(\delta) = \begin{bmatrix} \epsilon I & \frac{1}{2}\epsilon D & -\frac{1}{2}\epsilon I \\ \frac{1}{2}\epsilon D & D - \epsilon E(\delta) & \mathbb{0}_{n\times n} \\ -\frac{1}{2}\epsilon I & \mathbb{0}_{n\times n} & K \end{bmatrix} \tag{29}$$

and we defined the shorthand $E(\delta) = \mathrm{symm}(M\nabla^2 U(\delta))$ with $\mathrm{symm}(A) = \frac{1}{2}(A + A^{\mathrm{T}})$.

Authorized licensed use limited to: Johns Hopkins University. Downloaded on July 10,2020 at 16:04:53 UTC from IEEE Xplore. Restrictions apply.

We claim that for all δ, $H(\delta) > 0$. To see this, apply Lemma 12 from Appendix A to obtain $H(\delta) \geq H'(\delta)$ with

$$H'(\delta) := \begin{bmatrix} \frac{\epsilon}{2} I & \mathbb{0}_{n\times n} & \mathbb{0}_{n\times n} \\ \mathbb{0}_{n\times n} & D - \epsilon(E(\delta) + D^2) & \mathbb{0}_{n\times n} \\ \mathbb{0}_{n\times n} & \mathbb{0}_{n\times n} & K - \epsilon I \end{bmatrix}.$$

Given that D and K are positive-definite matrices, one can select ϵ to be positive yet sufficiently small so that $H'(\delta) > 0$.

To show exponential decline of the Lyapunov function $V(x)$, which is necessary for proving (26), we must find some positive constant α such that $\dot{V}(x) \leq -\alpha V(x)$.

We claim that a positive constant β_3, dependent on ρ from Assumption 2, exists such that $\|\chi\|^2 \geq \beta_3 \|x\|^2$. To see this, we note from Lemma 13 in Appendix A that a constant β_3' exists so that

$$\|\nabla U(\delta) - \nabla U(\bar{\delta})\|^2 \leq \beta_3' \|\delta - \delta^*\|^2. \tag{30}$$

The claim then follows with $\beta_3 = \min(1, {\beta_3'}^{-1})$.

In order to proceed, we set $\beta_4 := \min_{\mathcal{B}^{\mathrm{T}}\delta\in\Theta} \lambda_{\min}(H(\delta))$. Then, using (28), it follows that as far as $\mathcal{B}^{\mathrm{T}}\delta \in \Theta$

$$\dot{V}(x) \leq -\beta_4 \|\chi\|^2 \leq -\beta_3\beta_4 \|x\|^2 \leq -\frac{\beta_3\beta_4}{\beta_2} V =: -\alpha V(x)\,.$$

For this inequality to lead to the claimed exponential stability, we must guarantee that the solutions do not leave Θ. To do so, we study the sublevel sets of $V(x)$ and find one that is contained in Θ. Recall that the sublevel sets of $V(x)$ are invariant and thus solutions $x(t)$ are bounded for all $t \geq 0$ in sublevel sets $\{x : V(x) \leq V(x_0)\}$ for which $\mathcal{B}^{\mathrm{T}}\delta \in \Theta$. Hence, we require the initial conditions x_0 of solutions $x(t)$ to be within a suitable sublevel set $\{x : V(x) \leq V(x_0)\}$ where $\mathcal{B}^{\mathrm{T}}\delta \in \Theta$. We now construct such a sublevel set. Let

$$c := \beta_1 \frac{\xi^2}{\lambda_{\max}(\mathcal{B}\mathcal{B}^{\mathrm{T}})} \tag{31}$$

where $\xi > 0$ is a parameter with the property that any δ satisfying $\|\mathcal{B}^{\mathrm{T}}\delta - \mathcal{B}^{\mathrm{T}}\delta^*\| \leq \xi$ also satisfies $\mathcal{B}^{\mathrm{T}}\delta \in \Theta$. The parameter ξ exists because $\mathcal{B}^{\mathrm{T}}\delta^* \in \Theta$, and Θ is an open set. Accordingly, define the sublevel set $\Omega_c := \{x : V(x) \leq c\}$, with c defined above, and note that any point in Ω_c satisfies $\mathcal{B}^{\mathrm{T}}\delta \in \Theta$. As a matter of fact $V(x) \leq c$ implies $\|x\|^2 \leq \frac{\xi^2}{\lambda_{\max}(\mathcal{B}\mathcal{B}^{\mathrm{T}})}$ and therefore $\|\delta - \delta^*\|^2 \leq \frac{\xi^2}{\lambda_{\max}(\mathcal{B}\mathcal{B}^{\mathrm{T}})}$. This, in turn, implies that $\|\mathcal{B}^{\mathrm{T}}(\delta - \delta^*)\|^2 \leq \xi^2$, and hence $\mathcal{B}^{\mathrm{T}}\delta \in \Theta$ by the choice of ξ.

We conclude that any solution issuing from the sublevel set Ω_c will remain inside of it. Hence, along these solutions, the inequality $\dot{V}(x) \leq -\alpha V(x)$ always holds true.

By the comparison lemma [25, Lemma B.2], this inequality yields $V(x(t)) \leq e^{-\alpha t} V(x(0))$, which we combine again with (28) to arrive at (26) with $\lambda = \beta_2/\beta_1$.

Finally, we address the effect of K and T on α by introducing the scalar factors κ and τ multiplying K and T, and by studying the effect of manipulations of κ and τ on the exponential decline of $V(x)$ and, therefore, of $x(t)$. Note that α is a monotonically increasing function of $\beta_4 = \min_{\mathcal{B}^{\mathrm{T}}\delta\in\Theta} \lambda_{\min}(H(\delta))$. Recall that for any vector z, we have

$$\lambda_{\min}(H(\delta))\|z\|^2 \leq z^{\mathrm{T}} H(\delta) z$$

with equality if z is the eigenvector corresponding to $\lambda_{\min}(H(\delta))$. Let $e_{\min}$ denote the normalized eigenvector corresponding to $\lambda_{\min}(H(\delta))$. Then, for any vector z satisfying $\|z\| = 1$, $\lambda_{\min}(H(\delta)) = e_{\min}^{\mathrm{T}} H(\delta) e_{\min} \leq z^{\mathrm{T}} H(\delta) z$. Hence, we have

$$\beta_4 = \min_{\mathcal{B}^{\mathrm{T}}\delta\in\Theta} \lambda_{\min}(H(\delta)) = \min_{\mathcal{B}^{\mathrm{T}}\delta\in\Theta\,,\, z:\|z\|=1} z^{\mathrm{T}} H(\delta) z$$

where the last equality holds by noting that $e_{\min}$ is one of the vectors z at which the minimum is attained.

Now, suppose we multiply K by a factor $\kappa > 1$. Let $H'(\delta) = H(\delta) + \text{block diag}(\mathbb{0}, \mathbb{0}, (\kappa - 1)K)$. The new value of β_4 is given by

$$\beta_4' = \min_{\mathcal{B}^{\mathrm{T}}\delta\in\Theta\,,\, z:\|z\|=1} \underbrace{\left(z^{\mathrm{T}} H(\delta) z + \sum\nolimits_{i=1}^{n} (\kappa - 1) K_i z_{2n+i}^2 \right)}_{= z^{\mathrm{T}} H'(\delta) z}.$$

The argument of the minimization is not smaller than $z^{\mathrm{T}} H(\delta) z$ for any z. It follows that $\beta_4' \geq \min_{\mathcal{B}^{\mathrm{T}}\delta\in\Theta, z:\|z\|=1} z^{\mathrm{T}} H(\delta) z = \beta_4$. Similarly, if $0 < \kappa < 1$, then $\beta_4' \leq \min_{\mathcal{B}^{\mathrm{T}}\delta\in\Theta, z:\|z\|=1} z^{\mathrm{T}} H(\delta) z = \beta_4$. Hence, β_4 is a monotonically nondecreasing function of gain κ. Likewise, α is a monotonically decreasing function of β_2, which itself is a nondecreasing function of τ. ■

Theorem 7 is in line with the loop-shaping insight that the bandwidth K_i/T_i determines nominal performance: The decay rate α is monotonically nondecreasing in K_i/T_i.

C. Robustness Analysis

We now depart from nominal performance and focus on robustness. Recall a key disadvantage of pure integral control: It is not robust to biased measurement errors of the form (12). We now show that leaky integral control (13) is robust to such measurement errors. In what follows, instead of (13), consider leaky integral control subjected to the following measurement errors

$$u = -p \tag{32a}$$

$$T\dot{p} = \omega - K\,p + \eta \tag{32b}$$

where the measurement noise $\eta = \eta(t) \in \mathbb{R}^n$ is assumed to be an ∞-norm bounded disturbance. In this case, the bias-induced instability (see Section III-A) does not occur.

Let us first offer a qualitative steady-state analysis. For a constant vector η, the equilibrium equation (16c) becomes

$$\mathbb{0}_n = \omega^* - K\,p^* + \eta$$

so that the closed loop (1), (32) will admit synchronous equilibria. Indeed, the governing equations (17) determining the synchronous frequency ω_{sync} rewritten as

$$(D + K^{-1})\,\omega_{\text{sync}} \mathbb{1} = P^* - \nabla U(\theta^*) - K^{-1}\eta\,.$$

Observe that the noise terms η now take the same role as the constant injections P^*, and their effect can be made arbitrarily small by increasing K. We now make this qualitative steady-state reasoning more precise and derive a robustness criterion by means of the same Lyapunov approach used to prove Theorem 7. We take the measurement error η as disturbance input and quantify its effect on the convergence behavior along the lines of input-to-state stability. First, we define the specific robust stability criterion that we will use, adapted from [29].

Definition 1 (Input-to-state-stability with restrictions): A system $\dot{x} = f(x, \eta)$ is said to be input-to-state stable (ISS) with restriction $\mathcal{X}$ on $x(0) = x_0$ and restriction $\overline{\eta} \in \mathbb{R}_{>0}$ on $\eta(\cdot)$ if

Authorized licensed use limited to: Johns Hopkins University. Downloaded on July 10,2020 at 16:04:53 UTC from IEEE Xplore. Restrictions apply.

there exist a class $\mathcal{KL}$-function β and a class $\mathcal{K}_\infty$-function γ such that

$$\|x(t)\| \leq \beta(\|x_0\|, t) + \gamma(\|\eta(\cdot)\|_\infty)$$

for all $t \in \mathbb{R}_{\geq 0}$, $x_0 \in \mathcal{X}$, and inputs $\eta(\cdot) \in L_\infty^n$ satisfying

$$\|\eta(\cdot)\|_\infty := \operatorname*{ess\,sup}_{t \in \mathbb{R}_{\geq 0}} \|\eta(t)\| \leq \bar{\eta}.$$

Theorem 8 (ISS under biased leaky integral control): Consider system (23) in a closed loop with the biased leaky integral controller (32). Let Assumptions 1 and 2 hold true. Given a diagonal matrix $K > 0$, there exist a positive constant $\overline{\eta}$ and a set $\mathcal{X}$ such that the closed-loop system is ISS from the noise η to the state $x = \operatorname{col}(\delta - \delta^*, \omega - \omega^*, p - p^*)$ with restrictions $\mathcal{X}$ on x_0 and $\overline{\eta}$ on $\eta(\cdot)$, where $(\delta^*, \omega^*, p^*)$ is the equilibrium of the nominal system, i.e., with $\eta = 0$. In particular, the solutions $x(t) = \operatorname{col}(\delta(t) - \delta^*, \omega(t) - \omega^*, p(t) - p^*)$, with $(\delta(t), \omega(t), p(t))$ a solution to (23), (32) for which $x(0) \in \mathcal{X}$ and $\|\eta(\cdot)\|_\infty \leq \overline{\eta}$ are satisfied for all $t \in \mathbb{R}_{\geq 0}$, are given by

$$\|x(t)\|^2 \leq \lambda e^{-\hat{\alpha} t} \|x(0)\|^2 + \gamma \|\eta(\cdot)\|_\infty^2 \tag{33}$$

where $\hat{\alpha}$, λ, and γ are positive constants. Furthermore, when multiplying the gains K and T by the positive scalars κ and τ, respectively, then γ is monotonically decreasing (respectively, nonincreasing) as a function of κ (respectively, τ), and $\hat{\alpha}$ is monotonically nondecreasing as a function of κ and nonincreasing as a function of τ.

Proof: We start by extending the Lyapunov arguments from the proof of Theorem 7 to take the noise $\eta(t)$ into account, obtaining again an upper bound of $\dot{V}(x)$ in terms of $V(x)$.

From the proof of Theorem 7 recall the Lyapunov function derivative $\dot{V}(x) = -\chi^{\mathsf{T}} H(\delta) \chi - (p - p^*)^{\mathsf{T}} \eta$. Since for any positive parameter μ we have

$$-(p - p^*)^{\mathsf{T}} \eta \leq \mu \|p - p^*\|^2 + \frac{1}{\mu} \|\eta\|^2$$

one further obtains

$$\dot{V}(x) \leq -\chi^{\mathsf{T}} \underbrace{\left(H(\delta) - \begin{bmatrix} \mathbb{0} & \mathbb{0} & \mathbb{0} \\ \mathbb{0} & \mathbb{0} & \mathbb{0} \\ \mathbb{0} & \mathbb{0} & \mu I \end{bmatrix} \right)}_{= \hat{H}(\delta)} \chi + \frac{1}{\mu} \|\eta\|^2 .$$

Following the reasoning in the proof of Theorem 7, we note that $\hat{H}(\delta) \geq \hat{H}'(\delta)$, where

$$\hat{H}'(\delta) := \begin{bmatrix} \frac{\epsilon}{2} I & \mathbb{0}_{n \times n} & \mathbb{0}_{n \times n} \\ \mathbb{0}_{n \times n} & D - \epsilon(E(\delta) + D^2) & \mathbb{0}_{n \times n} \\ \mathbb{0}_{n \times n} & \mathbb{0}_{n \times n} & K - \epsilon I - \mu I \end{bmatrix}.$$

It follows that for sufficiently small values of ϵ and μ, $\hat{H}(\delta) \geq \hat{H}'(\delta) > 0$. To continue, let $\hat{\beta}_4 := \min_{\mathcal{B}^{\mathsf{T}} \delta \in \Theta} \lambda_{\min}(\hat{H}(\delta))$. As a result, we find that for a positive constant $\hat{\alpha} = \frac{\beta_3 \hat{\beta}_4}{\beta_2}$

$$\dot{V}(x) \leq -\hat{\alpha} V(x) + \frac{1}{\mu} \|\eta\|^2 \tag{34}$$

for all x such that $\mathcal{B}^{\mathsf{T}} \delta \in \Theta$.

We now again make sure that no solutions can leave the set Θ. To make this possible, it is necessary to impose a restriction on the magnitude of the noise $\bar{\eta}$ and the set of possible initial states, $\mathcal{X}$. In the remainder of the proof, we fix $\bar{\eta}$ such that

$$\bar{\eta}^2 = \hat{\alpha} c \mu$$

with c defined as in (31) in the proof of Theorem 7.

Define the sublevel set Ω_c, again as in the proof of Theorem 7. We now claim that the solutions of the closed-loop system cannot leave Ω_c. In fact, on the boundary $\partial\Omega_c$ of the sublevel set Ω_c, the right-hand side of (34) equals $-\hat{\alpha} c + \frac{1}{\mu} \|\eta\|^2$, which is a nonpositive constant by the choice of $\bar{\eta}$. Hence, a solution leaving Ω_c would contradict the property that $\dot{V}(x) \leq 0$ for all $x \in \partial\Omega_c$. We conclude that all solutions must satisfy (34) for all $t \in \mathbb{R}_{\geq 0}$. Hence, we choose $\mathcal{X} = \Omega_c$.

Having validated (34), we now derive the exponential bound (33). By the Comparison Lemma, the use of convolution integral and bounding $\|\eta(t)\|^2$ by $\|\eta(\cdot)\|_\infty^2$, we arrive at

$$V(x(t)) \leq e^{-\hat{\alpha} t} V(x_0) + \frac{1}{\hat{\alpha} \mu} \|\eta(\cdot)\|_\infty^2.$$

We combine this inequality with (28) and (30) to arrive at (33) with $\lambda = \beta_2 / \beta_1$ and $\gamma = (\hat{\alpha} \beta_1 \mu)^{-1}$.

Finally, we address the effects of K and T on $\hat{\alpha}$ and γ by introducing the scalar factors κ and τ multiplying K and T.

As κ increases, there is no need to increase ϵ, while it is possible to increase μ. Analogously to the reasoning in the proof of Theorem 7, increasing the value of κ for constant ϵ and increasing μ cannot lower the value of $\hat{\beta}_4$ and $\hat{\alpha}$, but decreases the value of γ. If one *decreases* κ, but multiplies μ by the same factor so as to keep $\hat{\beta}_4$ constant, μ will also decrease. This guarantees $\hat{\alpha}$ remains constant in this case, preserving its status as a nondecreasing function of κ. However, a decrease in μ results in an increase in γ, retaining its status as a decreasing function of κ. Therefore, $\hat{\alpha}$ is nondecreasing as a function of κ and γ is decreasing.

As in Theorem 7, τ affects only β_1 and β_2, and the same result holds true: $\hat{\alpha}$ is a monotonically nonincreasing function of τ. Analogously, γ is monotonically nonincreasing in τ. ■

Theorem 8 shows that larger gains K (and T) reduce (respectively, do not amplify) the effect of the noise η on the state x. This further emphasizes the tradeoff between frequency banding and controller performance already touched on in Section IV-A. We further extend and formalize this tradeoff in Section V-D by means of an $\mathcal{H}_2$ performance analysis.

Remark 2 (Exponential ISS with restrictions): The $\mathcal{KL}$–function from the ISS inequality (33) is an exponential function, so the stability property is in fact exponential ISS with restrictions. The need to include restrictions $\mathcal{X}$ on the initial conditions and $\bar{\eta}$ on the noise is due to the requirement of maintaining the state response within the safety region Θ. ■

D. $\mathcal{H}_2$ Performance Analysis

All findings thus far show that the closed-loop performance crucially depends on the choice of K_i and T_i. Small gains K_i are advantageous for steady-state properties, large gains K_i and T_i are advantageous for noise rejection, and the nominal performance does not deteriorate when increasing K_i/T_i. To further understand this tradeoff we now study the transient performance in the presence of stochastic disturbances by means of the $\mathcal{H}_2$ norm. The use of the $\mathcal{H}_2$ norm for evaluating power network performance was first introduced in [30]. This versatile framework allows us to characterize various network properties such

Authorized licensed use limited to: Johns Hopkins University. Downloaded on July 10,2020 at 16:04:53 UTC from IEEE Xplore. Restrictions apply.

as resistive power losses [30], voltage deviations [31], the role of inertia [32], and phase coherence [33], in the presence of stochastic disturbances, and network-wide frequency transients induced by step changes [34], [35].

Here, in a stochastic setting, we investigate the effect of the gains K and T on the steady-state frequency variance in the presence of power disturbances and noisy frequency measurements modeled as white noise inputs. More precisely, we compute the $\mathcal{H}_2$ norm of the system (15) with output $\omega(t)$ and inputs in (15b) and (15c). With this aim, we first linearize (15) around a steady state $(\theta^*, \omega^*, p^*)$.[2] Using $\nabla^2 U(\theta^*) = L_B$, where L_B is a weighted Laplacian matrix [22], and redefining (θ, ω, p) as a deviation from steady state, the closed-loop model (15) becomes

$$\begin{aligned} \dot{\theta} &= \omega \\ M\dot{\omega} &= -D\omega - L_B\theta - p \\ T\dot{p} &= \omega - Kp\,. \end{aligned}$$

We use $S_\zeta \zeta$ to denote the disturbances on the net power injection and $S_\eta \eta$ to model the noise incurred in the frequency measurement required to implement the controller (13). Then, by defining the system output as $y = \omega$, we obtain the linear time-invariant (LTI) system as

$$\begin{aligned} \begin{bmatrix} \dot{\theta} \\ \dot{\omega} \\ \dot{p} \end{bmatrix} &= \underbrace{\begin{bmatrix} 0 & I & 0 \\ -M^{-1}L_B & -M^{-1}D & -M^{-1} \\ 0 & T^{-1} & -T^{-1}K \end{bmatrix}}_{=A} \begin{bmatrix} \theta \\ \omega \\ p \end{bmatrix} \\ &\quad + \underbrace{\begin{bmatrix} 0 & 0 \\ M^{-1}S_\zeta & 0 \\ 0 & T^{-1}S_\eta \end{bmatrix}}_{=B} \begin{bmatrix} \zeta \\ \eta \end{bmatrix}, \; y = \underbrace{[0\; I\; 0]}_{=C} \begin{bmatrix} \theta \\ \omega \\ p \end{bmatrix}. \end{aligned} \tag{35}$$

The signals $\zeta \in \mathbb{R}^n$ and $\eta \in \mathbb{R}^n$ represent white noise with unit variance, i.e., $E[\zeta(t)^{\mathrm{T}}\zeta(\tau)] = \delta(t-\tau)I_n$ and $E[\eta(t)^{\mathrm{T}}\eta(\tau)] = \delta(t-\tau)I_n$, and $S_\zeta = \mathrm{diag}\{\sigma_{\zeta,i}, i \in \{1,\dots,n\}\}$, $S_\eta = \mathrm{diag}\{\sigma_{\eta,i}, i \in \{1,\dots,n\}\}$.

We are interested in understanding the effects of K_i and T_i on the system performance. To this aim, we will compute the $\mathcal{H}_2$ norm of (35) and compare it with that of the pure integrator, as well as the open loop system. From (14), we see that for $K_i \searrow 0$ (respectively, for $K_i \nearrow \infty$) for $i \in \{1,\dots,n\}$ we recover the closed-loop system controlled by pure integral control (7) (respectively, the open-loop system). Thus, in what follows, we denote the LTI system (35) by G_{leaky}, for $K = \mathbb{0}_{n\times n}$ by $G_{\text{integrator}}$, and for $K_i \nearrow \infty$ by $G_{\text{open-loop}}$.

The squared $\mathcal{H}_2$ norm of the LTI system (35) is given by

$$\|G\|_{\mathcal{H}_2}^2 = \lim_{t\to\infty} E[y^{\mathrm{T}}(t)y(t)]. \tag{36}$$

Via the observability Gramian X, $\|G\|_{\mathcal{H}_2}^2$ can be computed as

$$\|G\|_{\mathcal{H}_2}^2 = \mathrm{tr}(B^{\mathrm{T}}XB) \tag{37}$$

where X solves the Lyapunov equation

$$A^{\mathrm{T}}X + XA = -C^{\mathrm{T}}C. \tag{38}$$

[2]Of course, care must be taken when interpreting the results in this section since the steady-state itself depends on the controller gain K (see Section IV-A), but here we are merely interested in the transient performance.

Although a closed-form solution of (37) is generally hard to calculate, it is possible to provide a qualitative analysis by assuming homogeneous parameters as in the following result.

Theorem 9 ($\mathcal{H}_2$ norm of leaky integrator): Consider the LTI power system model G_{leaky} in (35). Assume homogeneous parameters, i.e., $M_i = m$, $D_i = d$, $T_i = \tau$, $K_i = k$, $\sigma_{\zeta,i} = \sigma_\zeta$, and $\sigma_{\eta,i} = \sigma_\eta$, $\forall i \in \{1,\dots,n\}$. Then, the squared $\mathcal{H}_2$ norm of G_{leaky} is given by

$$\begin{aligned} &\|G_{\text{leaky}}\|_{\mathcal{H}_2}^2 \\ &= \frac{n\sigma_\zeta^2}{2md} + \sum_{i=1}^{n} \frac{-\frac{k}{d}\sigma_\zeta^2 + \sigma_\eta^2}{2d\left[mk^2 + \left(\frac{m}{d} + d\tau\right)k + \tau + \lambda_i\tau^2\right]}\,. \end{aligned} \tag{39}$$

In particular, setting $k = 0$ in (39) gives

$$\|G_{\text{integrator}}\|_{\mathcal{H}_2}^2 = \frac{n\sigma_\zeta^2}{2md} + \sum_{i=1}^{n} \frac{\sigma_\eta^2}{2d\left(\tau + \lambda_i\tau^2\right)} \tag{40}$$

where $G_{\text{integrator}}$ denotes the linearized power system model controlled by the pure integral controller (7).

Proof: Consider the orthonormal change of input, state, and output variables $\theta = U\theta'$, $\omega = U\omega'$, $p = Up'$, $y = Uy'$, $\zeta = U\zeta'$, and $\eta = U\eta'$, where U is the orthonormal transformation that diagonalizes L_B: $U^T L_B U = \mathrm{diag}\{\lambda_1,\dots,\lambda_n\}$ with λ_i being the ith eigenvalue of L_B in increasing order ($\lambda_1 = 0 < \lambda_2 \le \cdots \le \lambda_n$). The $\mathcal{H}_2$ norm is invariant under this transformation and (35) decouples into n subsystems as

$$\begin{aligned} \begin{bmatrix} \dot{\theta}_i' \\ \dot{\omega}_i' \\ \dot{p}_i' \end{bmatrix} &= \underbrace{\begin{bmatrix} 0 & 1 & 0 \\ -\frac{\lambda_i}{m} & -\frac{d}{m} & -\frac{1}{m} \\ 0 & \frac{1}{\tau} & -\frac{k}{\tau} \end{bmatrix}}_{=A_i} \begin{bmatrix} \theta_i' \\ \omega_i' \\ p_i' \end{bmatrix} + \underbrace{\begin{bmatrix} 0 & 0 \\ \frac{\sigma_\zeta}{m} & 0 \\ 0 & \frac{\sigma_\eta}{\tau} \end{bmatrix}}_{=B_i} \begin{bmatrix} \eta_{p,i}' \\ \eta_{\omega,i}' \end{bmatrix} \\ y_i' &= \underbrace{[0\;1\;0]}_{=C_i} \begin{bmatrix} \theta_i' \\ \omega_i' \\ p_i' \end{bmatrix}. \end{aligned} \tag{41}$$

Then, based on (37) and (38), $\|G_{\text{leaky}}\|_{\mathcal{H}_2}^2$ can be calculated by computing the norm of the n subsystems (41) (see, e.g., [30], [32], [36]–[38]). The key step is to solve n Lyapunov equations

$$A_i^{\mathrm{T}}Q + QA_i = -C_i^{\mathrm{T}}C_i \tag{42}$$

where Q must be symmetric and can thus be parameterized as

$$Q = \begin{bmatrix} q_{11} & q_{12} & q_{13} \\ q_{12} & q_{22} & q_{23} \\ q_{13} & q_{23} & q_{33} \end{bmatrix}. \tag{43}$$

Whenever $\lambda_i \neq 0$ (42) has a unique solution Q. For $\lambda_1 = 0$, the system (41) has a zero pole that could render infinite $\mathcal{H}_2$ norm and nonunique solutions to (42). We will later see that this mode is unobservable and thus the $\mathcal{H}_2$ norm is finite.

Authorized licensed use limited to: Johns Hopkins University. Downloaded on July 10,2020 at 16:04:53 UTC from IEEE Xplore. Restrictions apply.

We now focus on the case $\lambda_i \neq 0$. Direct calculations show that

$$q_{11} = \frac{\lambda_i}{d}\left(-\frac{km}{\tau^2}q_{33} + \frac{1}{2}\right) - \frac{\lambda_i}{\tau}q_{33} \tag{44a}$$

$$q_{12} = 0 \tag{44b}$$

$$q_{13} = \lambda_i q_{33} \tag{44c}$$

$$q_{22} = \frac{m}{d}\left(-\frac{km}{\tau^2}q_{33} + \frac{1}{2}\right) \tag{44d}$$

$$q_{23} = -\frac{km}{\tau}q_{33} \tag{44e}$$

where all solutions are parameterized in

$$q_{33} = \frac{1}{2d\left[\frac{m}{\tau^2}k^2 + \left(\frac{m}{d\tau^2} + \frac{d}{\tau}\right)k + \frac{1}{\tau} + \lambda_i\right]}\,. \tag{45}$$

Therefore, we obtain

$$\|G_{\text{leaky},i}\|_{\mathcal{H}_2}^2 = \operatorname{tr}(B_i^{\mathrm{T}} Q B_i) = \left(\frac{\sigma_\zeta}{m}\right)^2 q_{22} + \frac{\sigma_\eta^2}{\tau^2}q_{33}\,. \tag{46}$$

By substituting (44d) and (45) into (46), we arrive at

$$\|G_{\text{leaky},i}\|_{\mathcal{H}_2}^2 = \frac{\frac{k}{\tau^2}\left(-\frac{\sigma_\zeta^2}{d} + \frac{\sigma_\eta^2}{k}\right)}{2d\left[\frac{m}{\tau^2}k^2 + \left(\frac{m}{d\tau^2} + \frac{d}{\tau}\right)k + \frac{1}{\tau} + \lambda_i\right]} + \frac{\sigma_\zeta^2}{2md}\,. \tag{47}$$

We now consider the case $\lambda_i = 0$, i.e., $i = 1$. Since $\lambda_1 = 0$, neither $\dot{\omega}_1'$, nor $\dot{p}_1'$, nor y_1' depends on θ_1' in (41). Thus, θ_i' is not observable, and we can simplify the system (41) to

$$\begin{bmatrix}\dot{\omega}_i' \\ \dot{p}_i'\end{bmatrix} = \underbrace{\begin{bmatrix}-\frac{d}{m} & -\frac{1}{m} \\ \frac{1}{\tau} & -\frac{k}{\tau}\end{bmatrix}}_{=A_i}\begin{bmatrix}\omega_i' \\ p_i'\end{bmatrix} + \underbrace{\begin{bmatrix}\frac{\sigma_\zeta}{m} & 0 \\ 0 & \frac{\sigma_\eta}{\tau}\end{bmatrix}}_{=B_i}\begin{bmatrix}\eta_{p,i}' \\ \eta_{\omega,i}'\end{bmatrix}$$

$$y_i' = \underbrace{[1\ 0]}_{C_i}\begin{bmatrix}\omega_i' \\ p_i'\end{bmatrix}.$$

Again, we solve the Lyapunov equation (42), but here $Q = Q^{\mathrm{T}}$ is a 2-by-2 matrix. A similar calculation as before yields that $\|G_{\text{leaky},1}\|_{\mathcal{H}_2}^2$ is also given by (47) with $\lambda_1 = 0$. Therefore, $\|G_{\text{leaky}}\|_{\mathcal{H}_2}^2 = \sum_{i=1}^n \|G_{\text{leaky},i}\|_{\mathcal{H}_2}^2$, which is equal to (39).

Finally, note from (7) and (13) that the leaky integrator reduces to an integrator when $K = \mathbb{0}_{n\times n}$. It follows that $\|G_{\text{integrator}}\|_{\mathcal{H}_2}^2$ can be obtained by setting $k = 0$ in (39). ■

Theorem 9 provides an explicit expression for the closed-loop $\mathcal{H}_2$ performance under leaky integral control (13) as well as under pure integral control (7). Observe from (37), (39), and (40) that power disturbances and measurement noise have an independent additive effect on the $\mathcal{H}_2$ norm. Thus, either of the two effects can be obtained by setting $\sigma_\eta = 0$ or $\sigma_\zeta = 0$.

The following corollary, whose proof is in Appendix B1, shows the supremacy of leaky integral control over pure integral control for any positive gain k. Furthermore, in the presence of only measurement noise, increasing k or τ always improves $\|G_{\text{leaky}}\|_{\mathcal{H}_2}^2$ which is consistent with the ISS insights obtained from Theorem 8.

Corollary 10 (Monotonicity of the $\mathcal{H}_2$ norm): Under the assumptions of Theorem 9, for any $k > 0$ the closed-loop $\mathcal{H}_2$ norm under leaky integral control is strictly smaller than that under pure integral control: $\|G_{\text{leaky}}\|_{\mathcal{H}_2}^2 < \|G_{\text{integrator}}\|_{\mathcal{H}_2}^2$. Moreover, in the absence of power disturbances, $\sigma_\zeta = 0$, $\|G_{\text{leaky}}\|_{\mathcal{H}_2}^2$ is a strictly decreasing function of $k \geq 0$ and $\tau \geq 0$.

Remark 3 (Optimal $\mathcal{H}_2$ performance at open loop): Observe from (39) that in the absence of power disturbances ($\sigma_\zeta = 0$) and in the presence of measurement noise ($\sigma_\eta \neq 0$), the optimal gains are $k \nearrow \infty$ or $\tau \nearrow \infty$, which from (14) reduces to the open-loop case. This insight is consistent with the noise rejection bounds (33) in Theorem 8. Of course, the steady-state characteristics in Section IV-A all demand a sufficiently small value of k, and power disturbances will typically be present as well. Nevertheless, these considerations pose the question of whether leaky integral control can ever improve the open-loop performance $\|G_{\text{open-loop}}\|_{\mathcal{H}_2}^2 := n\sigma_\zeta^2/(2md)$ obtained for $k, \tau \nearrow \infty$. We explicitly address this question below. ■

The next corollary (for proof, see Appendix B2) will use the characterization of the effect of τ on the performance as a mechanism to derive an optimal choice for both k and τ that can ensure the improvement of the leaky integrator performance $\|G_{\text{leaky}}\|_{\mathcal{H}_2}$ not only with respect to the pure integrator performance $\|G_{\text{integrator}}\|_{\mathcal{H}_2}$ but also with respect to the open-loop performance $\|G_{\text{open-loop}}\|_{\mathcal{H}_2}$.

Corollary 11 ($\mathcal{H}_2$ optimal tuning): Under the assumption of Theorem 9 and for any $\tau > 0$, and k such that

$$\frac{k}{d} > \left(\frac{\sigma_\eta}{\sigma_\zeta}\right)^2 \tag{48}$$

the closed-loop performance under the leaky integral control outperforms the open-loop system performance, i.e.,

$$\|G_{\text{leaky}}\|_{\mathcal{H}_2}^2 < \|G_{\text{open-loop}}\|_{\mathcal{H}_2}^2.$$

Moreover, the global minimum of the $\mathcal{H}_2$ norm under leaky integral control is obtained by setting $\tau \to \tau^* = 0$ and k to

$$k^* = d\left(\frac{\sigma_\eta}{\sigma_\zeta}\right)^2\left(1 + \sqrt{1 + \left(\frac{\sigma_\zeta}{d}\right)^2}\right). \tag{49}$$

Remark 4 (Necessity of condition (48)): We highlight that condition (48) is, in fact, necessary for improving performance beyond $\|G_{\text{open-loop}}\|_{\mathcal{H}_2}$. When (48) is violated, $\frac{\partial}{\partial\tau}\|G_{\text{leaky}}\|_{\mathcal{H}_2}^2 < 0$; see Appendix B2. In this case, if (48) does not hold, it is easy to see from (39) that $\|G_{\text{leaky}}\|_{\mathcal{H}_2} \searrow \|G_{\text{open-loop}}\|_{\mathcal{H}_2}$ as $\tau \nearrow \infty$, which implies $\|G_{\text{leaky}}\|_{\mathcal{H}_2} > \|G_{\text{open-loop}}\|_{\mathcal{H}_2}$. ■

Corollary 11 suggests that the optimal controller tuning requires $\tau^* = 0$, which reduces the leaky integrator to a proportional droop controller with gain $1/k^*$. However, setting τ to small values reduces the response time $T_i/K_i = \tau/k$ of the leaky integrator, which in an actual implementation will be limited by the actuator's response time (not modeled here). We point out, however, that Corollary 11 also shows that the leaky integrator provides performance improvements for any $\tau > 0$, and thus this limitation will only affect the extent to which the $\mathcal{H}_2$ performance is improved.

The optimal value k^* in (49) also unveils interesting tradeoffs between performance and robustness. More precisely, on the one hand, in the high-power disturbance regime $\sigma_\zeta \nearrow \infty$, the optimal gain is $k^* \searrow 0$. The latter choice of course weakens the robustness properties described in Section IV-B. On the other hand, in the presence of large measurement errors $\sigma_\eta \nearrow \infty$, one

Authorized licensed use limited to: Johns Hopkins University. Downloaded on July 10,2020 at 16:04:53 UTC from IEEE Xplore. Restrictions apply.

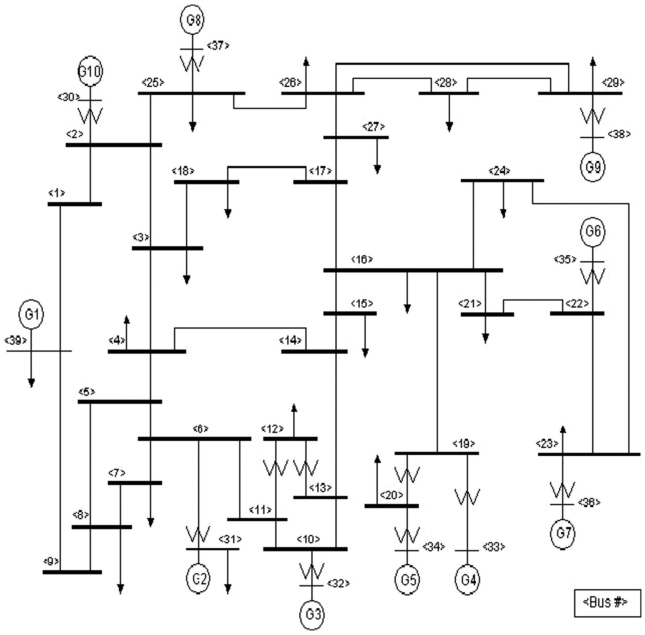

Fig. 1. 39-bus New England system used in simulations.

loses the ability to properly regulate the frequency as $k^* \nearrow \infty$, i.e., the open-loop case.

Remark 5 (Joint banded frequency restoration and optimal $\mathcal{H}_2$ performance): This last discussion also unveils a critical tradeoff of leaky integral control: It may be infeasible to jointly satisfy (20) and (48) when the measurement noise σ_η is large. For a specified level ε of frequency restoration, the parameter k that satisfies (20), or equivalently

$$k \leq \left(\frac{|\sum_i P_i^*|}{n\varepsilon} - d \right)^{-1}$$

may not satisfy (48) and thus leads to worse performance than that of open loop. Of course, one can still take large values of τ to mitigate this degradation, as in Remark 3. However, this comes at the cost of lower convergence rate: Large τ leads to slow feedback. We refer to Section VI for further discussion of these tradeoffs. ■

V. Case Study: IEEE 39 New England System

In this section, we perform a case study with the 39-bus New England system (see Fig. 1), which is modeled as in (1)–(2) with parameters M_i (for the 10 generator buses), V_i, and B_{ij} taken from [39]. The inertia coefficients M_i are set to zero for the 29 (load) buses without generators. Note that M_i's in our simulations are heterogeneous, which relaxes our simplifying assumption in Section IV-D that M_i's are homogeneous and allows for testing the proposed scheme under a more realistic setting. For every generator bus i, the damping coefficient D_i is chosen as 20 per unit (p.u.) so that a 0.05 p.u. (3 Hz) change in frequency will cause a 1 p.u. (1000 MW) change in the generator output power. For every load bus i, D_i is chosen as 1/200 of that of a generator. Note that the generator turbine-governor dynamics are ignored in the model (1)–(2) leading to a simulated frequency response that is faster than in practice, but the fundamental dynamics of the system are retained for a proof-of-concept illustration of the proposed controller. For all simulations below, a 300-MW step increase in active-power load occurs at each of buses 15, 23, and 39 at time $t = 5\,\mathrm{s}$.

A. Comparison Between Controllers Without Noise

We implement each of the following controllers across the 10 generators to stabilize the system after the increase in load.

1) *Distributed-averaging based integral control* (DAI):

$$u = -p \tag{50a}$$

$$T\dot{p} = A^{-1}\omega - LAp\,. \tag{50b}$$

Here, $L = L^{\mathsf{T}}$ is the Laplacian matrix of a communication graph among the controllers, which we choose as a ring graph with uniform weights 0.1. The matrix A is diagonal with entries $A_{ii} = a_i$ being the cost coefficients in (4a) chosen as 1.0 for generators G3, G5, G6, G9, and G10, and 2.0 for the rest. We choose the time constant $T_i = 0.05\,\mathrm{s}$ for every generator i. The DAI control (50) is known to achieve stable and optimal frequency regulation as in Problem 2; see [7]–[12]. Even though DAI control is based on a reliable and fast communication environment, we include it here as a baseline for comparison purposes.

2) *Decentralized pure integral control* (7) with time constant $T_i = 0.05\,\mathrm{s}$ for every generator i.

3) *Decentralized leaky integral control* (13) with time constant $T_i = 0.05\,\mathrm{s}$ for every generator i. The gain K_i equals 0.005 for generators G3, G5, G6, G9, and G10, and 0.01 for the rest. The values of K_i are proportional to the values of a_i in DAI (50) so that the dispatch objectives (4a) and (22a) are identical.

Fig. 2 (dashed plots) shows the frequency at G1 (all other generators display similar frequency trends), and Fig. 3 shows the active-power outputs of all generators, under the different controllers above and without noisy measurements. First, note that all closed-loop systems reach stable steady-states; see Theorems 2 and 8. Second, observe from Fig. 2 that both pure integral and DAI control can perfectly restore the frequencies to the nominal value, whereas leaky integral control leads to a steady-state frequency error as predicted in Lemma 3. Third, as observed from Fig. 3, both DAI and leaky integral control achieve the desired asymptotic power sharing (2:1 ratio between G3, G5, G6, G9, G10 and other generators) as predicted in Corollary 5. However, leaky integral control solves the dispatch problem (22) thereby underestimating the net load compared to DAI, which solves (4); see Corollary 6. We conclude that fully decentralized leaky integral controller can achieve a performance similar to the communication-based DAI controller—though at the cost of steady-state offsets in both frequency and power adjustment.

B. Comparison Between Controllers With Noise

Next, a noise term $\eta_i(t)$ is added to the frequency measurements ω in (50b), (7b), and (13b) for DAI, pure integral, and leaky integral control, respectively. The noise $\eta_i(t)$ is sampled from a uniform distribution on $[0, \overline{\eta}_i]$, with $\overline{\eta}_i$ selected such that the ratios of $\overline{\eta}_i$ between generators are $1:2:3:\cdots:10$ and $\|[\overline{\eta}_1, \overline{\eta}_2, \dots]\| = \overline{\eta} = 0.01\,\mathrm{Hz}$. The meaning of $\overline{\eta}$ here is consistent with that in Definition 1 and Theorem 8. At each generator i, the noise has nonzero mean $\overline{\eta}_i/2$ (inducing a constant measurement bias) and variance $\sigma_{\eta,i}^2 = \overline{\eta}_i^2/12$.

Authorized licensed use limited to: Johns Hopkins University. Downloaded on July 10,2020 at 16:04:53 UTC from IEEE Xplore. Restrictions apply.

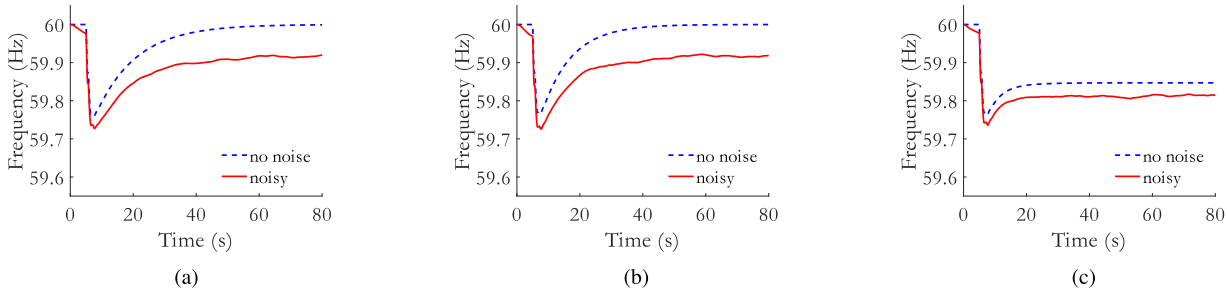

Fig. 2. Frequency at generator G1 under different control methods. (a) DAI control. (b) Decentralized pure integral control. (c) Leaky integral control.

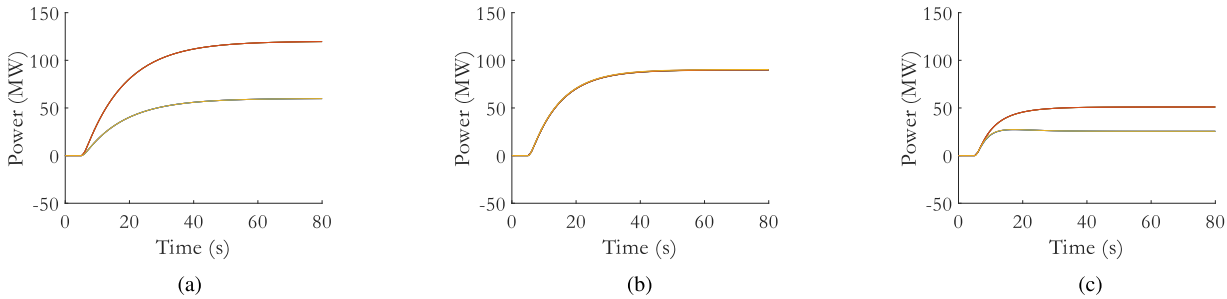

Fig. 3. Changes in active-power outputs of all the generators without noise. (a) DAI control. (b) Decentralized pure integral control. (c) Leaky integral control.

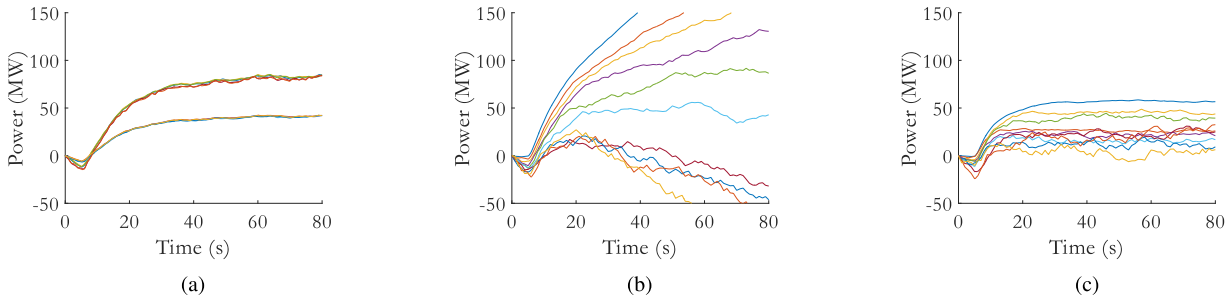

Fig. 4. Changes in active-power outputs of all the generators, under a frequency measurement noise bounded by $\overline{\eta} = 0.01\,\mathrm{Hz}$. (a) DAI control. (b) Decentralized pure integral control. (c) Leaky integral control.

Fig. 2 (solid plots) shows the frequency at generator G1, and Fig. 4 shows the changes in active-power outputs of all the generators under such a measurement noise. Observe from Fig. 2(b)–(c) and Fig. 4(b)–(c) that leaky integral control is more robust to measurement noise than pure integral control. Fig. 4(a) and (c) show that DAI control is even more robust than the leaky integral control in terms of generator power outputs, which is not surprising since the averaging process between neighboring DAI controllers can effectively mitigate the effect of noise—thanks to communication.

C. Impacts of Leaky Integral Control Parameters

Next, we investigate the impacts of inverse dc gains K_i and time constants T_i on the performance of leaky integral control.

First, we set the integral time constant $T_i = \tau = 0.05\,\mathrm{s}$ for every generator i, and tune the gains $K_i = k$ for generators G3, G5, G6, G9, and G10; $K_i = 2k$ for other generators to ensure the same asymptotic power sharing as above. The following metrics of controller performance are calculated for the frequency at generator G1:

1) the steady-state frequency error without noise;

2) the convergence time without noise, which is defined as the time when frequency error enters and stays within $[0.95, 1.05]$ times its steady-state;

3) the frequency root-mean-square-error (RMSE) from its nominal steady-state, calculated over 60–80 s (the average RMSE over 100 random realizations is taken).

The RMSE results from measurement noise $\eta_i(t)$ generated every second at every generator i from a uniform distribution on $[-\overline{\eta}_i, \overline{\eta}_i]$, where the meaning of $\overline{\eta}_i$ is the same as that in Section V-B; $\eta_i(t)$ has zero mean so that the performance in mitigating steady-state bias and noise-induced variance can be observed separately. Fig. 5 shows these metrics as functions of k. It can be observed that the steady-state error increases with k, as predicted by Lemma 3; convergence is faster as k increases, in agreement with Theorem 7; and robustness to measurement noise is improved as k increases, as predicted by Theorem 8 and Corollary 10.

Authorized licensed use limited to: Johns Hopkins University. Downloaded on July 10,2020 at 16:04:53 UTC from IEEE Xplore. Restrictions apply.

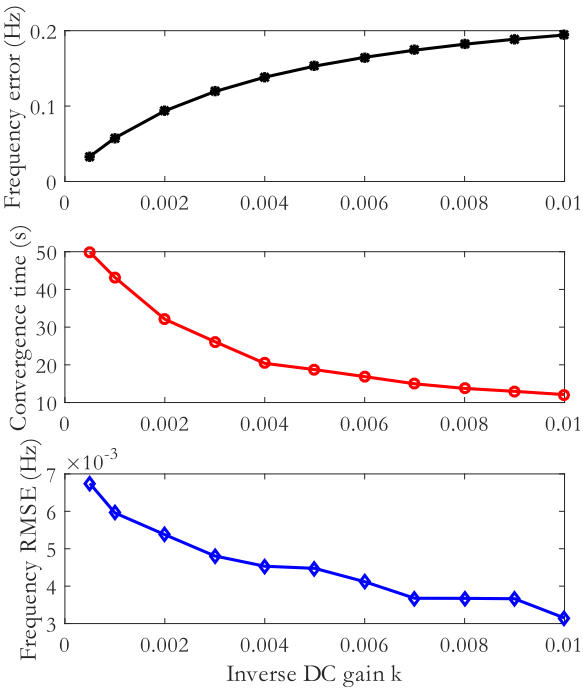

Fig. 5. Steady-state error (upper), convergence time (middle), and RMSE (lower) of frequency at generator G1, as functions of the gain k for leaky integral control. The time constants are $T_i = \tau = 0.05\,\mathrm{s}$ for all generators.

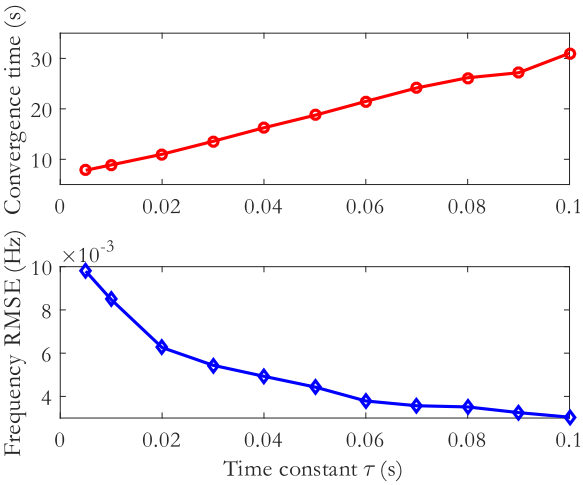

Fig. 6. Convergence time (upper) and RMSE (lower) of frequency at generator G1, as functions of the time constant $T_i = \tau$ for leaky integral control. The gains K_i are 0.005 for G3, G5, G6, G9, G10 and 0.01 for other generators.

Next, we tune the integral time constants $T_i = \tau$ for all generators and fix $k = 0.005$, i.e., $K_i = 0.005$ for G3, G5, G6, G9, G10 and $K_i = 0.01$ for other generators, for a balance between steady-state and transient performance. Since the steady-state is independent of τ, only the convergence time (measured for the case without noise) and RMSE (taken as the average of 100 runs with different realizations of noise) of frequency at generator G1 are shown in Fig. 6. It can be observed that convergence is faster as τ decreases, which is in line with Theorem 7. Robustness to measurement noise is improved as τ increases, which is in line with Theorem 8 and predicted by Corollary 10.

Finally, we discuss performance degradation if the response time of leaky integral controller is smaller than the actuation response time. The generator turbine-governor dynamics can be modeled as first- or second-order transfer functions, with dominant time constants in the range of $[0.25\,\mathrm{s}, 2.5\,\mathrm{s}]$ for hydraulic turbines and $[4\,\mathrm{s}, 7\,\mathrm{s}]$ for steam turbines [40, Ch. 9]. The analogous time constant for our controller corresponds to the parameter ratio T_i/K_i. For the simulations in Figs. 2–4, this ratio was chosen as $10\,\mathrm{s}$ for generators G3, G5, G6, G9, G10 and of $5\,\mathrm{s}$ for others. Thus, they are compatible with actuation through steam and hydraulic turbines. If this was not the case, the controllers have to be slowed down and their performance can be inferred using Figs. 5 and 6. Finally, we stress that the proven robustness guarantees, i.e., input-to-state-stability of the nonlinear model, will not be at stake, provided that the initial conditions and the maximum noise magnitude are those characterized in the proof of Theorem 8.

D. Tuning Recommendations

Our results quantifying the effects of the gains K and T on the system behavior lead to a number of insights about tuning the gains in a practical setting. Specifically, a possible approach is as follows. First, the ratios between the values K_i^{-1} can be determined using Corollary 5 and knowledge about the generator operation cost. Second, a lower bound on the sum of these values $\sum_{i=1}^n K_i^{-1}$ can be obtained from Corollary 4 according to the required steady-state performance. Since by Theorem 7 larger gains K_i are beneficial to faster convergence, it is preferable to set the values of K_i^{-1} equal to the lower bound from Corollary 4. Note that in Corollary 4, the value of ε is normally specified in the grid code and is thus assumed to be known. The grid code also specifies a worst-case power imbalance $\sum_{i=1}^n P_i^*$ that frequency controllers have to counteract before the system is redispatched. Specifically, in our simulations, we assumed an admissible frequency deviation $\varepsilon = 0.3\,\mathrm{Hz} = 0.005\,\mathrm{p.u.}$, a worst-case power imbalance $\sum_{i=1}^n P_i^* = 1800\,\mathrm{MW} = 18\,\mathrm{p.u.}$ (approximately the simultaneous loss of the two largest generators), and $\sum_{i=1}^n D_i = 2100\,\mathrm{p.u.}$ based on practical generator droop settings and load damping values. As a result of Corollary 4, we obtained $\sum_{i=1}^n K_i^{-1} = 1500\,\mathrm{p.u.}$, which together with Corollary 5 leads to our choice of $K_i = 0.005$ for generators G3, G5, G6, G9, G10 and 0.01 for the others. Third, with the inverse gains K_i^{-1} fixed, the time constants T_i can be determined to strike a desired tradeoff between frequency convergence rate and noise rejection. We outline two possible approaches in the following based on Theorem 8 or simulation data.

A possible approach to determine T_i is foreshadowed by the proof of Theorem 8. The maximum noise magnitude $\bar{\eta}$ (for which input-to-state stability can be established in Theorem 8) is linear in β_1/β_2, which are both defined as functions of T in the proof of Lemma 14. From their definitions, one learns that $\bar{\eta}$ is a convex function of each of the values of T. By requiring that the value of $\bar{\eta}$ exceeds the sensor noise estimate, one can then find bounds on the values of T_i. Within these bounds one should select the lowest values of T_i, as this is both beneficial for a faster convergence rate $\hat{\alpha}$ and a smaller deviation due to the disturbance $\gamma\bar{\eta}^2$, as seen in the proof of Theorem 8.

If the system under investigation makes the above considerations for T infeasible, an alternative tuning approach for T

Authorized licensed use limited to: Johns Hopkins University. Downloaded on July 10,2020 at 16:04:53 UTC from IEEE Xplore. Restrictions apply.

relies on simulation data. For example, consider the simplified case presented in Fig. 6, where there is a single time constant $\tau = T_i$ for all the generators i to be tuned. By means of regression methods, one can approximate the relationships between the frequency convergence time T_{conv}, the frequency RMSE f_{RMSE}, and the gain τ via the functions

$$T_{\mathrm{conv}}(\tau) = a\tau + b$$
$$f_{\mathrm{RMSE}}(\tau) = ce^{-\alpha\tau} + d$$

where $a > 0$, $b \in \mathbb{R}$, $c > 0$, $d \in \mathbb{R}$, $\alpha > 0$ are constants. The time constant τ can then be chosen according to the criterion

$$\min_{\tau \geq 0} \quad \gamma\, T_{\mathrm{conv}}(\tau) + f_{\mathrm{RMSE}}(\tau)$$

where $\gamma > 0$ is a tradeoff parameter selected according to the relative importance of convergence time and noise robustness. The unique optimal solution to this tradeoff criterion is

$$\tau^* = \max\left\{\frac{1}{\alpha}\log\left(\frac{\alpha c}{\gamma a}\right), 0\right\}.$$

VI. Summary and Discussion

In the following, we summarize our findings and the various tradeoffs that need to be taken into account for the tuning of the proposed leaky integral controller (13).

From the discussion following the Laplace-domain representation (14), the gains K_i and T_i of the leaky integral controller (13) can be understood as interpolation parameters for which the leaky integral controller reduces to a pure integrator ($K_i \searrow 0$) with gain T_i, a proportional (droop) controller ($T_i \searrow 0$) with gain K_i^{-1}, or no control action ($K_i, T_i \nearrow \infty$). Within these extreme parameterizations, we found the following tradeoffs: The steady-state analysis in Section IV-A showed that proportional power sharing and banded frequency regulation is achieved for any choice of gains $K_i > 0$: Their sum gives a desired steady-state frequency performance (see Corollary 4), and their ratios give rise to the desired proportional power sharing [see Corollary (5)]. However, a vanishingly small gain K_i is required for asymptotically exact frequency regulation (see Corollary 6), i.e., the case of integral control. Otherwise, the net load is always underestimated. On the one hand, in regard to stability, we inferred global stability for vanishing $K_i \searrow 0$ (see Theorem 2) but also an absence of robustness to measurement errors as in (12). On the other hand, for positive gains $K_i > 0$ we obtained nominal local exponential stability (see Theorem 7) with exponential rate as a function of K_i/T_i and robustness (in the form of exponential ISS with restrictions) to bounded measurement errors (see Theorem 8) with increasing (respectively, nondecreasing) robustness margins to measurement noise as K_i (or T_i) becomes larger. From a $\mathcal{H}_2$-performance perspective, we could qualitatively (under homogeneous parameter assumptions) confirm these results for the linearized system. In particular, we showed that measurement disturbances are increasingly suppressed for larger gains K_i and T_i (see Corollary 10), but for sufficiently large power disturbances a particular choice of gains K_i together with sufficiently small time constants T_i optimizes the transient performance (see Corollary 11), i.e., the case of droop control.

Our findings, especially the last one, pose the question whether the leaky integral controller (13) actually improves upon proportional (droop) control (the case $T_i = 0$) with sufficiently large droop gain K_i^{-1}. The answers to this question can be found in practical advantages: 1) leaky integral control obviously low-pass filters measurement noise; 2) has a finite bandwidth thus resulting in a less aggressive control action more suitable for slowly ramping generators; and 3) is not susceptible to windup (indeed, a PI control action with anti-windup reduces to a lag element [19]). 4) Other benefits that we did not touch upon in our analysis are related to classical loop shaping, e.g., the frequency for the phase shift can be specified for leaky integral control (13) to give a desired phase margin (and thus also practically relevant delay margin) where needed for robustness or overshoot.

In summary, our lag-element-inspired leaky integral control is fully decentralized, stabilizing, and can be tuned to achieve robust noise rejection, satisfactory steady-state regulation, and a desirable transient performance with exponential convergence. We showed that these objectives are not always aligned, and tradeoffs have to be found. Our tuning recommendations are summarized in Section V-D. From a practical perspective, we recommend to tune the leaky integral controller toward robust steady-state regulation and to address transient performance with related lead-element-inspired controllers [38].

We believe that the aforementioned extension of the leaky integrator with lead compensators is a fruitful direction for future research. Another relevant direction is a rigorous analysis of decentralized integrators with dead-zones that are often used by practitioners (in power systems and beyond) as alternatives to finite-dc-gain implementations, such as the leaky integrator. Finally, all the presented results can and should be extended to more detailed higher-order power system models.

Appendix

A. Technical Lemmas

We recall several technical lemmas used in the main text.

Lemma 12 (Matrix cross terms): [12, Lemma 15] Given any four matrices A, B, C, and D of appropriate dimensions, we have

$$M := \begin{bmatrix} A & B^{\mathrm{T}}C \\ C^{\mathrm{T}}B & D \end{bmatrix} \geq \begin{bmatrix} A - B^{\mathrm{T}}B & 0 \\ 0 & D - C^{\mathrm{T}}C \end{bmatrix} =: M'.$$

Lemma 13 (Bounding the potential function): [12, Lemma 5] Consider the Bregman distance $V_\delta := U(\delta) - U(\bar{\delta}) - \nabla U(\bar{\delta})^{\mathrm{T}}(\delta - \delta^*)$. The following properties hold for all $\delta, \bar{\delta}$ that satisfy $B^{\mathrm{T}}\delta, B^{\mathrm{T}}\bar{\delta} \in \Theta$.

1) There exist positive scalars α_1 and α_2 such that

$$\alpha_1\|\delta - \delta^*\| \leq \|\nabla U(\delta) - \nabla U(\delta^*)\| \leq \alpha_2\|\delta - \delta^*\|.$$

2) There exist positive scalars α_3 and α_4 such that

$$\alpha_3\|\delta - \delta^*\|^2 \leq V_\delta \leq \alpha_4\|\delta - \delta^*\|^2.$$

Lemma 14 (Positivity of V): Suppose that Assumption 2 holds true and $B^{\mathrm{T}}\delta \in \Theta$. The Lyapunov function V in (27) satisfies

$$\beta_1\|x\|^2 \leq V(x) \leq \beta_2\|x\|^2$$

for some positive constants β_1 and β_2, with x given in (25), provided that ϵ is sufficiently small.

Authorized licensed use limited to: Johns Hopkins University. Downloaded on July 10,2020 at 16:04:53 UTC from IEEE Xplore. Restrictions apply.

Proof: This proof follows the same line of arguments as the proof of [12, Lemma 8], but accounts for our slightly different Lyapunov function. We will bound $V(x)$ in (27) term-by-term. The quadratic terms in $\omega-\omega^*$ and $p-p^*$ are easily bounded in terms of the eigenvalues of matrices M and T, respectively. The terms in δ and δ^* is addressed in the second statement of Lemma 13. These three terms lead to the early bound

$$\begin{aligned}\min(\lambda_{\min}(M),\lambda_{\min}(T),\alpha_3)\|x\|^2 &\le V(x)|_{\epsilon=0}\\ &\le \max(\lambda_{\max}(M),\lambda_{\max}(T),\alpha_4)\|x\|^2.\end{aligned}$$

The cross term $\epsilon(\nabla U(\delta)-\nabla U(\delta^*))^{\mathrm{T}}M\omega$ can be written as

$$\begin{pmatrix}\nabla U(\delta)-\nabla U(\delta^*)\\ \omega\end{pmatrix}^{\mathrm{T}}\begin{bmatrix}\mathbb{0} & \frac{\epsilon}{2}M\\ \frac{\epsilon}{2}M & \mathbb{0}\end{bmatrix}\begin{pmatrix}\nabla U(\delta)-\nabla U(\delta^*)\\ \omega\end{pmatrix}.$$

This allows us to apply Lemma 12, which yields the

$$\begin{aligned}-\|\nabla U(\delta)-\nabla U(\delta^*)\|^2-\lambda_{\max}(M)^2\|\omega\|^2&\\ \le(\nabla U(\delta)-\nabla U(\delta^*))^{\mathrm{T}}M\omega&\\ \le\|\nabla U(\delta)-\nabla U(\delta^*)\|^2+\lambda_{\max}(M)^2\|\omega\|^2.&\end{aligned}$$

By applying the first statement of Lemma 13, we can bound the entire Lyapunov function using

$$\begin{aligned}\beta_1&=\min(\lambda_{\min}(M)-\epsilon\lambda_{\max}(M)^2,\lambda_{\min}(T),\alpha_3-\epsilon\alpha_2^2)\\ \beta_2&=\max(\lambda_{\max}(M)+\epsilon\lambda_{\max}(M)^2,\lambda_{\max}(T),\alpha_4+\epsilon\alpha_2^2).\end{aligned}$$

Finally, we select ϵ sufficiently small so that $\beta_1>0$. ■

B. Proof of Corollaries

We provide here the proof of Corollaries 10 and 11.

1) Proof of Corollary 10:

Proof: For a given value of τ, consider the function

$$f(k)=n\alpha_6+\sum_{i=1}^{n}\frac{-\alpha_1 k+\alpha_2}{\alpha_3k^2+\alpha_4k+\alpha_5(\lambda_i)} \tag{51}$$

where $\alpha_1=\sigma_\zeta^2/d$, $\alpha_2=\sigma_\eta^2$, $\alpha_3=2dm$, $\alpha_4=2d\,(m/d+d\tau)$, $\alpha_5(\lambda_i)=2d(\tau+\lambda_i\tau^2)$, and $\alpha_6=\sigma_\zeta^2/2md$ are all positive parameters. The function $f(k)$ interpolates between $\|G_{\text{leaky}}\|_{\mathcal{H}_2}^2=f(k)$ and $\|G_{\text{integrator}}\|_{\mathcal{H}_2}^2=f(0)$.

We prove that if either power disturbances σ_ζ or measurement noise σ_η equals zero, then $\|G_{\text{leaky}}\|_{\mathcal{H}_2}^2<\|G_{\text{integrator}}\|_{\mathcal{H}_2}^2$ holds true for all $k>0$. In presence of only measurement noise, i.e., when $\sigma_\zeta=0$ the function $f(k)$ reduces to

$$f_\eta(k)=\sum_{i=1}^{n}\frac{\alpha_2}{\alpha_3k^2+\alpha_4k+\alpha_5(\lambda_i)} \tag{52}$$

whose derivative with respect to k is

$$f_\eta'(k)=-\sum_{i=1}^{n}\frac{\alpha_2(2\alpha_3k+\alpha_4)}{(\alpha_3k^2+\alpha_4k+\alpha_5(\lambda_i))^2}\,. \tag{53}$$

Clearly, for all $k>0$, $f_\eta'(k)<0$. An analogous reasoning holds true when analyzing $\|G_{\text{leaky}}\|_{\mathcal{H}_2}^2$ as a function of τ, which shows the second claimed statement. Furthermore, $f_\eta'(k)<0$ also implies that $\|G_{\text{leaky}}\|_{\mathcal{H}_2}^2=f_\eta(k)<f_\eta(0)=\|G_{\text{integrator}}\|_{\mathcal{H}_2}^2$

If only power disturbances are applied, i.e., when $\sigma_\eta=0$ in (39) and (40), then $f(k)$ reduces to

$$f_\zeta(k)=n\alpha_6-\sum_{i=1}^{n}\frac{\alpha_1 k}{\alpha_3k^2+\alpha_4k+\alpha_5(\lambda_i)}. \tag{54}$$

Clearly, for all $k>0$, $\|G_{\text{leaky}}\|_{\mathcal{H}_2}^2=f_\zeta(k)<f_\zeta(0)=\|G_{\text{integrator}}\|_{\mathcal{H}_2}^2$. Therefore, since $\|G_{\text{leaky}}\|_{\mathcal{H}_2}^2=f(k)=f_\zeta(k)+f_\eta(k)$, it follows for all $k>0$ that $\|G_{\text{leaky}}\|_{\mathcal{H}_2}^2=f_\eta(k)+f_\zeta(k)<f_\eta(0)+f_\zeta(0)=\|G_{\text{integrator}}\|_{\mathcal{H}_2}^2$. ■

2) Proof of Corollary 11:

Proof: First notice that for $\sigma_\eta^2-\sigma_\zeta^2k/d>0$, the first term of (39) is always positive and thus $\|G_{\text{leaky}}\|_{\mathcal{H}_2}>\|G_{\text{open loop}}\|_{\mathcal{H}_2}$ for all τ. As a result, one can only improve the performance beyond open loop when $\sigma_\eta^2-\sigma_\zeta^2k/d<0$, which is equivalent to (48). The derivative of (39) with respect to τ equals

$$\frac{\partial}{\partial\tau}\|G_{\text{leaky}}\|_{\mathcal{H}_2}^2=\sum_{i=1}^{n}\frac{-(\sigma_\eta^2-\frac{k}{d}\sigma_\zeta^2)2d(2\tau\lambda_i+1)}{(2d[mk^2+(\frac{m}{d}+d\tau)k+\tau+\lambda_i\tau^2])^2}.$$

Therefore, $\frac{\partial}{\partial\tau}\|G_{\text{leaky}}\|_{\mathcal{H}_2}^2>0$ whenever (48) holds true. It follows that the minimal norm is the limit when $\tau=0$.

We now compute the derivative of $f_\zeta(k)$ as

$$f_\zeta'(k)=\sum_{i=1}^{n}\frac{\alpha_1(\alpha_3k^2-\alpha_5(\lambda_i))}{(\alpha_3k^2+\alpha_4k+\alpha_5(\lambda_i))^2}\,. \tag{55}$$

Notice that $\tau=0$ implies $\alpha_5(\lambda_i)=\tau(1+\lambda_i\tau)=0$ so that

$$f_\zeta'(k)\big|_{\tau=0}=\sum_{i=1}^{n}\frac{\alpha_1(\alpha_3k^2)}{(\alpha_3k^2+\alpha_4k)^2}\,.$$

Thus, when considering f_η and f_ζ for $\tau=0$, we get

$$\begin{aligned}f'(k)\big|_{\tau=0}&=f_\eta'(k)\big|_{\tau=0}+f_\zeta'(k)\big|_{\tau=0}\\ &=n\frac{\alpha_1\alpha_3k^2-2\alpha_2\alpha_3k-\alpha_2\alpha_4}{(\alpha_3k^2+\alpha_4k)^2}\,.\end{aligned}$$

By setting $f'(k)\big|_{\tau=0}=0$, the optimal value of k is obtained as the unique positive root of the second-order polynomial

$$\begin{aligned}p(k)&=\alpha_1\alpha_3k^2-2\alpha_2\alpha_3k-\alpha_2\alpha_4\\ &=2m\left(\sigma_\zeta^2k^2-2d\sigma_\eta^2k-\sigma_\eta^2\right)\end{aligned}$$

which is explicitly given by (49). ■

ACKNOWLEDGMENT

The authors would like to thank D. Groß for various helpful discussions that improved the presentation of this paper.

REFERENCES

[1] J. Machowski, J. W. Bialek, and J. R. Bumby, *Power System Dynamics*. 2nd ed., Hoboken, NJ, USA: Wiley, 2008.
[2] H. Bevrani, *Robust Power System Frequency Control*, vol. 85. New York, NY, USA: Springer-Verlag, 2009.
[3] D. K. Molzahn *et al.*, "A survey of distributed optimization and control algorithms for electric power systems," *IEEE Trans. Smart Grid*, vol. 8, no. 6, pp. 2941–2962, Nov. 2017.
[4] F. Dörfler and S. Grammatico, "Gather-and-broadcast frequency control in power systems," *Automatica*, vol. 79, pp. 296–305, 2017.

Authorized licensed use limited to: Johns Hopkins University. Downloaded on July 10,2020 at 16:04:53 UTC from IEEE Xplore. Restrictions apply.

[5] M. Andreasson, D. V. Dimarogonas, H. Sandberg, and K. H. Johansson, "Distributed control of networked dynamical systems: Static feedback, integral action and consensus," *IEEE Trans. Autom. Control*, vol. 59, no. 7, pp. 1750–1764, Jul. 2014.
[6] Q. Shafiee, J. M. Guerrero, and J. Vasquez, "Distributed Secondary Control for Islanded MicroGrids – A Novel Approach," *IEEE Trans. Power Electron.*, vol. 29, no. 2, pp. 1018–1031, 2014.
[7] C. Zhao, E. Mallada, and F. Dörfler, "Distributed frequency control for stability and economic dispatch in power networks," in *Proc. Amer. Control Conf.*, Chicago, IL, USA, Jul. 2015, pp. 2359–2364.
[8] F. Dörfler, J. W. Simpson-Porco, and F. Bullo, "Breaking the hierarchy: Distributed control & economic optimality in microgrids," *IEEE Trans. Control Netw. Syst.*, vol. 3, no. 3, pp. 241–253, Sep. 2016.
[9] C. De Persis, N. Monshizadeh, J. Schiffer, and F. Dörfler, "A Lyapunov approach to control of microgrids with a network-preserved differential-algebraic model," in *Proc. IEEE Conf. Decis. Control*, Las Vegas, NV, USA, Dec. 2016, pp. 2595–2600.
[10] S. Trip, M. Bürger, and C. De Persis, "An internal model approach to (optimal) frequency regulation in power grids with time-varying voltages," *Automatica*, vol. 64, pp. 240–253, 2016.
[11] M. Andreasson, D. V. Dimarogonas, H. Sandberg, and K. H. Johansson, "Distributed PI-control with applications to power systems frequency control," in *Proc. Amer. Control Conf.*, Portland, OR, USA, Jun. 2014, pp. 3183–3188.
[12] E. Weitenberg, C. De Persis, and N. Monshizadeh, "Exponential convergence under distributed averaging integral frequency control," *Automatica*, vol. 98, pp. 103–113, 2018.
[13] N. Li, C. Zhao, and L. Chen, "Connecting automatic generation control and economic dispatch from an optimization view," *IEEE Trans. Control Netw. Syst.*, vol. 3, no. 3, pp. 254–264, Sep. 2016.
[14] X. Zhang and A. Papachristodoulou, "A real-time control framework for smart power networks: Design methodology and stability," *Automatica*, vol. 58, pp. 43–50, 2015.
[15] C. Zhao, E. Mallada, S. H. Low, and J. W. Bialek, "A unified framework for frequency control and congestion management," in *Proc. Power Syst. Comput. Conf.*, 2016, pp. 1–7.
[16] E. Mallada, C. Zhao, and S. Low, "Optimal load-side control for frequency regulation in smart grids," *IEEE Trans. Autom. Control*, vol. 62, no. 12, pp. 6294–6309, Dec. 2017.
[17] N. Ainsworth and S. Grijalva, "Design and quasi-equilibrium analysis of a distributed frequency-restoration controller for inverter-based microgrids," in *Proc. North Amer. Power Symp.*, Manhattan, KS, USA, Sep. 2013, pp. 1–6.
[18] J. Schiffer, R. Ortega, C. A. Hans, and J. Raisch, "Droop-controlled inverter-based microgrids are robust to clock drifts," in *Proc. Amer. Control Conf.*, Chicago, IL, USA, Jul. 2015, pp. 2341–2346.
[19] G. F. Franklin, J. D. Powell, and A. Emami-Naeini, *Feedback Control of Dynamic Systems*, vol. 2. Reading, MA, USA: Addison-Wesley, 1994.
[20] R. Heidari, M. M. Seron, and J. H. Braslavsky, "Ultimate boundedness and regions of attraction of frequency droop controlled microgrids with secondary control loops," *Automatica*, vol. 81, pp. 416–428, 2017.
[21] Y. Han *et al.*, "Analysis of washout filter-based power sharing strategy–An equivalent secondary controller for islanded microgrid without LBC lines," *IEEE Trans. Smart Grid*, vol. 9, no. 5, pp. 4061–4076. 2018.
[22] F. Bullo, *Lectures on Network Systems*, 1 Ed., with contributions by J. Cortes, F. Dörfler, and S. Martinez, 2018. [Online]. Available: http://motion.me.ucsb.edu/book-lns
[23] J. M. Guerrero, J. C. Vasquez, J. Matas, L. G. de Vicuna, and M. Castilla, "Hierarchical control of droop-controlled AC and DC microgrids–A general approach toward standardization," *IEEE Trans. Ind. Electron.*, vol. 58, no. 1, pp. 158–172, Jan. 2011.
[24] A. J. Wood and B. F. Wollenberg, *Power Generation, Operation, and Control*, 2nd ed. Hoboken, NJ, USA: Wiley, 1996.
[25] H. K. Khalil, *Nonlinear Control*. M. J. Horton, Ed. London, U.K.: Pearson, 2014.
[26] P. J. Campo and M. Morari, "Achievable closed-loop properties of systems under decentralized control: Conditions involving the steady-state gain," *IEEE Trans. Autom. Control*, vol. 39, no. 5, pp. 932–943, May 1994.
[27] K. J. Åström and T. Hägglund, *Advanced PID Control*. Pittsburgh, PA, USA: ISA-The Instrumentation, Systems and Automation Society, 2006.
[28] P. W. Sauer and M. A. Pai, *Power System Dynamics and Stability*. Hoboken, NJ, USA: Wiley, 1998.
[29] A. R. Teel, "A nonlinear small gain theorem for the analysis of control systems with saturation," *IEEE Trans. Autom. Control*, vol. 41, no. 9, pp. 1256–1270, Sep. 1996.
[30] E. Tegling, B. Bamieh, and D. Gayme, "The price of synchrony: Evaluating the resistive losses in synchronizing power networks," *IEEE Trans. Control Netw. Syst.*, vol. 2, no. 3, pp. 254–266, Sep. 2015.
[31] M. Andreasson, E. Tegling, H. Sandberg, and K. H. Johansson, "Performance and scalability of voltage controllers in multi-terminal HVdc networks," in *Proc. Amer. Control Conf.*, May 2017, pp. 3029–3034.
[32] B. K. Poolla, S. Bolognani, and F. Dorfler, "Optimal placement of virtual inertia in power grids," *IEEE Trans. Autom. Control*, vol. 62, no. 12, pp. 6209–6220, Dec. 2017.
[33] E. Tegling, M. Andreasson, J. W. Simpson-Porco, and H. Sandberg, "Improving performance of droop-controlled microgrids through distributed pi-control," in *Proc. Amer. Control Conf.*, Jul. 2016, pp. 2321–2327.
[34] M. Andreasson, E. Tegling, H. Sandberg, and K. H. Johansson, "Coherence in synchronizing power networks with distributed integral control," in *Proc. IEEE 56th Annu. Conf. Decis. Control*, Dec. 2017, pp. 6327–6333.
[35] F. Paganini and E. Mallada, "Global performance metrics for synchronization of heterogeneously rated power systems: The role of machine models and inertia," in *Proc. 55th Annu. Allerton Conf. Commun., Control, Comput.*, Oct. 2017, pp. 324–331.
[36] A. Mešanović, U. Münz, and C. Heyde, "Comparison of $\mathcal{H}_\infty$, $\mathcal{H}_2$, and pole optimization for power system oscillation damping with remote renewable generation," *IFAC-PapersOnLine*, vol. 49, no. 27, pp. 103–108, 2016.
[37] M. Pirani, J. W. Simpson-Porco, and B. Fidan, "System-theoretic performance metrics for low-inertia stability of power networks," Mar. 2017, arXiv:1703.02646.
[38] Y. Jiang, R. Pates, and E. Mallada, "Performance tradeoffs of dynamically controlled grid-connected inverters in low inertia power systems," in *Proc. IEEE 56th Conf. Decis. Control*, 2017, pp. 5098–5105.
[39] K. W. Cheung, J. Chow, and G. Rogers, "Power system toolbox, v 3.0.," *Rensselaer Polytechnic Inst. Cherry Tree Sci. Softw.*, vol. 48, p. 53, 2009.
[40] P. Kundur, *Power System Stability and Control*. New York, NY, USA: McGraw-Hill, 1994.

Erik Weitenberg received the B.Sc. degree in mathematics and the M.Sc. degree in mathematics with a specialization in algebra and cryptography, in 2010 and 2012, respectively, from the University of Groningen, Groningen, The Netherlands, where he is currently working toward the Ph.D. degree in control of cyber-physical systems.

His current research interests include stability and robustness of networked and cyberphysical systems, with applications to power systems.

Yan Jiang received the B.Eng. degree in electrical engineering and automation from Harbin Institute of Technology, Harbin, China, in 2013, and the M.S. degree in electrical engineering from Huazhong University of Science and Technology, Wuhan, China, in 2016. She is currently working toward the Ph.D. degree at the Department of Electrical and Computer Engineering and the M.S.E. degree at the Department of Applied Mathematics and Statistics, Johns Hopkins University, Baltimore, MD, USA.

Her research interests include the area of control of power systems.

Authorized licensed use limited to: Johns Hopkins University. Downloaded on July 10,2020 at 16:04:53 UTC from IEEE Xplore. Restrictions apply.

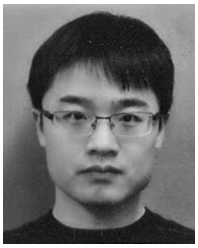

Changhong Zhao (S'12–M'15) received the B.Eng. degree in automation from Tsinghua University, Beijing, China, in 2010, and the Ph.D. degree in electrical engineering from California Institute of Technology, Pasadena, CA, USA, in 2016.

He is a Researcher with the National Renewable Energy Laboratory, Golden, CO, USA. His research interests include distributed control of networked systems, power system dynamics and stability, and optimization of power and multienergy systems.

Dr. Zhao was a recipient of the Caltech Demetriades-Tsafka-Kokkalis Ph.D. Thesis Prize, the Caltech Charles Wilts Ph.D. Thesis Prize, and the 2015 Qualcomm Innovation Fellowship Finalist Award.

Enrique Mallada (S'09–M'13) received the Ingeniero en Telecomunicaciones degree from Universidad ORT, Montevideo, Uruguay, in 2005, and the Ph.D. degree in electrical and computer engineering with a minor in applied mathematics from Cornell University, Ithaca, NY, USA, in 2014.

He is an Assistant Professor of electrical and computer engineering with Johns Hopkins University, Baltimore, MD, USA. Prior to joining Johns Hopkins University in 2016, he was a Postdoctoral Fellow with the Center for the Mathematics of Information, Caltech from 2014 to 2016. His research interests include the areas of control, dynamical systems and optimization, with applications to engineering networks such as power systems and the Internet.

Prof. Mallada was recipient of the CAREER Award from the National Science Foundation (NSF) in 2018, the ECE Director's Ph.D. Thesis Research Award for his dissertation in 2014, the Center for the Mathematics of Information (CMI) Fellowship from Caltech in 2014, and the Cornell University Jacobs Fellowship in 2011.

Claudio De Persis received the Laurea degree in electronic engineering in 1996 and the Ph.D. degree in system engineering in 2000, both from the University of Rome "La Sapienza," Rome, Italy.

He is a Professor with the Engineering and Technology Institute, Faculty of Science and Engineering, University of Groningen, the Netherlands. Previously, he held faculty positions with the Department of Mechanical Automation and Mechatronics, University of Twente, and the Department of Computer, Control, and Management Engineering, University of Rome "La Sapienza". He was a Research Associate with the Department of Systems Science and Mathematics, Washington University, St. Louis, MO, USA, in 2000–2001, and with the Department of Electrical Engineering, Yale University, New Haven, CT, USA, in 2001–2002. His main research interest is in control theory, and his recent research interests include dynamical networks, cyberphysical systems, smart grids, and resilient control.

Prof. Persis was an Editor for the *International Journal of Robust and Nonlinear Control* (2006–2013), an Associate Editor for the IEEE TRANSACTIONS ON CONTROL SYSTEMS TECHNOLOGY (2010–2015), and for the IEEE TRANSACTIONS ON AUTOMATIC CONTROL (2012–2015). He is currently an Associate Editor for the *Automatica* (2013-present) and for the IEEE CONTROL SYSTEMS LETTERS (2017-present).

Florian Dörfler received his Ph.D. degree in Mechanical Engineering from the University of California at Santa Barbara in 2013, and a Diplom degree in Engineering Cybernetics from the University of Stuttgart in 2008.

He is an Assistant Professor with the Automatic Control Laboratory, ETH Zürich, Zurich, Switzerland. From 2013 to 2014, he was an Assistant Professor with the University of California Los Angeles. His primary research interests include distributed control, complex networks, and cyberphysical systems currently with applications in energy systems.

Prof. Dörfler is a recipient of the 2009 Regents Special International Fellowship, the 2011 Peter J. Frenkel Foundation Fellowship, and the 2015 UCSB ME Best Ph.D. Award. His students were recipients or finalists for Best Student Paper Awards at the 2013 European Control Conference, the 2016 American Control Conference, and the 2017 PES PowerTech Conference. His articles received the 2010 ACC Student Best Paper Award, the 2011 O. Hugo Schuck Best Paper Award, the 2012–2014 Automatica Best Paper Award, and the 2016 IEEE Circuits and Systems Guillemin-Cauer Best Paper Award.

Authorized licensed use limited to: Johns Hopkins University. Downloaded on July 10,2020 at 16:04:53 UTC from IEEE Xplore. Restrictions apply.